

Urban atmospheric humidity excesses and deficits in two Mexican metropolises: Guadalajara and Puebla

Adalberto TEJEDA-MARTÍNEZ^{1*}, Gabriel BALDERAS-ROMERO²,
Luz Elena MOREYRA-GONZÁLEZ³ and J. Omar CASTRO-DÍAZ¹

¹ Universidad Veracruzana, Xalapa, C.P. 91090, Veracruz, México.

² Departamento de Investigaciones Arquitectónicas y Urbanísticas, Benemérita Universidad Autónoma de Puebla, Puebla, C.P. 72000, Puebla, México.

³ Doctorado en Diseño Bioclimático, Universidad Autónoma Metropolitana Azcapotzalco, Azcapotzalco, C.P. 02200, Ciudad de México, México.

*Corresponding author: atejeda.martinez@gmail.com

RESUMEN

Los estudios que comparan la humedad atmosférica entre ambientes urbanos y suburbanos y urbanos-rurales son escasos; a la vez, los resultados de esos estudios son muy dispersos y poco concluyentes. En este artículo se comparan las diferencias de temperatura atmosférica, humedad relativa y humedad absoluta medidas en los límites entre el dosel urbano y la capa límite en dos metrópolis elevadas de México: Guadalajara y Puebla. Las variaciones de los contrastes de la humedad relativa entre distintos ambientes resultan inversamente proporcionales a las variaciones de temperatura. En Guadalajara predominan los excesos urbanos de humedad absoluta a partir de mayo y se mantienen hasta septiembre; en Puebla los contrastes urbanos-suburbanos son menores que en Guadalajara, siguen un ciclo diario y llegan a ser negativos entre el mediodía y las 18:00 hora local. Entre marzo y septiembre las diferencias urbanas-rurales en Puebla son positivas entre las 10:00 y las 18:00 hora local, y débiles en el periodo nocturno.

ABSTRACT

Comparative studies of atmospheric humidity between urban and suburban and urban-rural environments are scarce, and their results are very scattered and inconclusive. In this paper, we compare differences in atmospheric temperature, relative humidity and absolute humidity measured at the limits between the urban canopy and the boundary layer in two elevated metropolises in Mexico: Guadalajara and Puebla. Results show that variations in relative humidity contrasts between different environments have an inverse relationship with the temperature variations. In Guadalajara, the urban excesses of absolute humidity are predominant from May to September. In Puebla the urban-suburban contrasts are lower than in Guadalajara, following a daily cycle and being negative between noon and 18:00 LT. From March to September urban-rural differences in Puebla are positive between 10:00 and 18:00 LT, and weak during the nocturnal period.

Keywords: urban climate, urban atmospheric humidity, Guadalajara, Puebla.

1. Background

Publications on urban atmospheric humidity are fewer in quantity and much more recent than those on urbanization effects on atmospheric temperature, according to various authors throughout the years, and recently reiterated by Oke et al. (2017, chpt. 9),

Unger et al. (2018a) and Yang et al. (2020). Table SI in the supplementary material of the present paper is a compilation on the subject, reporting 46 papers published in more than five decades (1967 to 2021), less than one per year in average. As can be seen, the subject has not been trendy but is still relevant.

Figure 1a shows that more than 30% of the papers were published in the first decade of the 21st century; in the whole period (Fig. 1b), two thirds have been focused on middle and high latitudes, and two thirds on cities with more than 500 000 inhabitants (Fig. 1c). In 25% of the papers the hygrometric variable used (Fig. 1d) is relative humidity (RH), in 33% some variable measuring atmospheric vapor concentration (vapor pressure, specific humidity, mixing ratio, absolute humidity or dew point temperature) is utilized, and in the remaining 42% both variables are employed. Therefore, obtaining conclusions is not easy since the publications are very disparate in terms of geographical area, size of the cities and humidity variables analyzed (Oke et al., 2017). Moreover, in the appendices of 25% the articles the results clearly indicate an excess of urban moisture; another 25% report moisture deficits in the city, and the remaining

50% show that one situation occurs in certain periods and the opposite occurs in others.

The summarized results in Table SI are important contributions to the understanding of urban hygrometry, but only some of the most useful theoretical considerations for this paper will be highlighted.

The pioneering work of Chandler (1967) addressed humidity in the English city of Leicester, with 270 000 inhabitants at the time. He found that wind, temperature, cloud cover, evaporation rate, land use, and the size and occupancy of the city played important roles in the diurnal cycles of humidity variations. During the night, absolute humidity was higher in the city, while RH was always most of the time. However, the conclusions were not definitive due to the uncertainties of the measurement equipment, which propagated to the evaluations of the hydric differences among different environments.

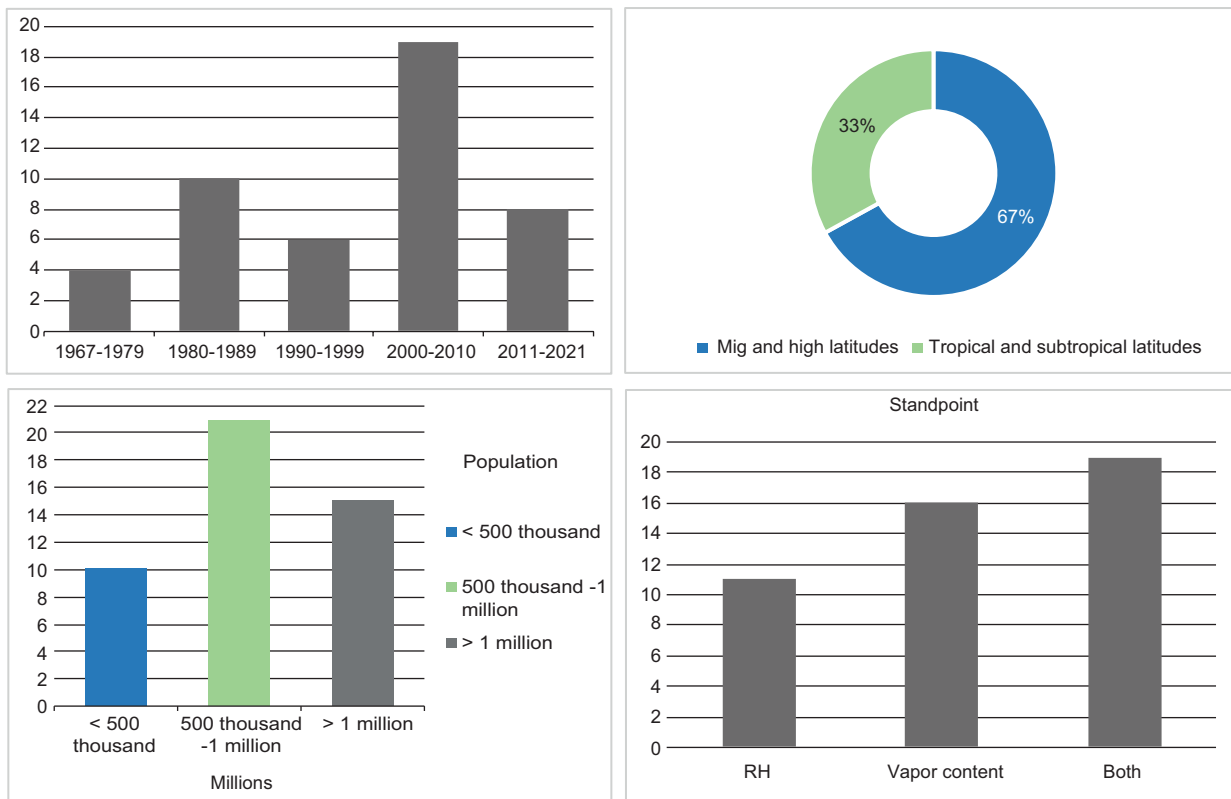


Fig. 1. Distribution of the research papers mentioned in Table SI of the supplementary material, according to (a) decade of publication, (b) latitude, (c) number of inhabitants of the corresponding cities, and (d) hydrological variable used (relative humidity [RH]) or vapor content)

Ackerman (1987) studied humidity contrasts in Chicago (3 000 000 inhabitants at the time) by comparing humidity data from urban and rural stations. He acknowledged that no single humidity variable is perfect for describing the phenomenon; for example, vapor pressure is a direct measure of humidity content in the atmosphere, but as air can hold less moisture at low temperatures, small differences in humidity during the cold season tend to be hidden, while RH is inversely dependent on temperature. Therefore, its behavior is strongly influenced by the urban heat island. Adebayo (1987) recognized that although the best variable to describe the effects of the city on atmospheric water vapor is not necessarily RH, its analysis is useful because of its implications for human health, comfort, and energy consumptions; thus, he used it to describe the case of Ibadam, Nigeria, and found that urban RH is lower by 2 to 10 percentage points (pp) relative to rural surroundings.

The research by Holmer and Eliasson (1999) on the Swedish city of Göteborg (approximately 600 000 inhabitants) has an original focus since they looked, with data from four years (1988, 1989, 1990, and 1994), for the impact of urban moisture excess on the urban heat island, particularly by the effects of water vapor on the longwave radiation balance and the latent heat fluxes between the surface and the atmosphere. They found that in warm summers with low precipitation the urban excess of vapor pressure was 3 hPa, while in other conditions it was only 1 hPa, and during several nights the urban moisture excess reached 7 hPa. Such anomalies were positively correlated with the intensity of the urban heat island, with the maximum of the island preceded by 2 to 5 h of maximum urban moisture excess.

Using vapor pressure, Unger (1999), Unger et al. (2018b) found that the Hungarian city of Szeged (approximately 150 000 inhabitants) was more humid almost the whole year during daytime, mainly due to artificial sources of urban humidity, which he analyzed through a dryness index. In contrast, through transects, Cuadrat et al. (2015) statistically related the urban dry island in the Spanish city of Zaragoza to geographical factors such as topography, land cover, and reflectivity from satellite images as well as prevailing wind patterns.

One of the most recent and diligent works is the one by Yang et al. (2020), who compared eight different

local climate zones (Stewart and Oke, 2012) in the city of Nanjing, China (approximately 7 000 000 inhabitants). They confirmed that the phenomenon is complex, as it depends on many factors such as synoptic conditions, urban morphology, thermal configuration of the city, vegetation and impervious canopies, water bodies, industrial water use, advection, cloud cover, turbulent anthropogenic moisture transfer, and single precipitation events. They affirmed that hygric fields cannot be discussed independently from thermal fields, and they found the nocturnal heat island is related to RH deficits and specific humidity excesses.

Oke et al. (2017, chpt. 9) remark on how limited the literature on the subject is, as mentioned above, and the difficulty of comparing studies using different humidity variables. According to the literature reviewed, the conclusion obtained by these authors is that the hypothetical causes of urban moisture excesses or deficits are not entirely clear for any city. They state that in middle and high latitudes during summer there is an urban moisture deficit in the diurnal period and an excess during the nocturnal period. The first one is mainly the result of a lower vapor pressure in the city due to its higher impermeability, which is exacerbated by a higher vertical transport and mixing in cities (due to their higher roughness and thermal turbulence) that enhance exchanges between near-surface air and drier air above the canopy (urban, suburban, or rural). At night, the urban moisture excess probably results from the decrease in dew formation due to the urban heat island and anthropogenic water vapor emissions.

Through a review of half a century of research on urban climates on (sub)tropical regions, Roth (2007) found a relatively small number of mostly descriptive studies that do not address the physical causes of urban climate phenomena. He considers that cities produce their own climates connected to the rest of the climate system by atmospheric chemistry and radiation balance, and that moisture in urban areas depends on artificial water supplements in the city, playing an important role in urban-rural differences in temperature and atmospheric humidity.

The research by Jáuregui and Tejada (1997) on the subject is the only one in Mexico. They found that Mexico City presented a lower specific humidity than its rural or suburban surroundings, but in some cases these differences were around the magnitude

of the instrumental uncertainty, so they cannot be considered as conclusive.

2. Study areas

This paper compares the urban effects on atmospheric humidity in two Mexican metropolitan areas, both tropical highlands: Guadalajara and Puebla. In Mexico, a metropolitan area is defined as an urban concentration of complete municipalities in a single unit that share a central city and are highly functionally interrelated, or an urban center with more than one million inhabitants even if it has not exceeded its municipal limit, or cross-border urban centers with more than 250 000 inhabitants (SEMARNAT, 2020). Since the study areas do not cover the total surface of the officially called metropolitan areas, but exceed the limits of the cities that give them a name, and for the sake of conciseness, in this article they will be called metropolis of Guadalajara and Puebla, or simply Guadalajara or Puebla.

To classify urban, suburban, and rural environments, the study areas were selected according to their distance from the metropolis center. While the urban zone in Puebla is located inside the so-called historical center, in Guadalajara it is 5 km away. Both suburban areas are located within the periphery of the metropolises.

Since both metropolises have expanded without strategic urban planning and have mostly grown horizontally, structures and building materials between urban and suburban environments do not differ significantly. Differences can be seen in the metabolism of each zone with variations in land use, building density and vehicular flow rates with saturations at different hours of the day. In addition, vegetations present differences in their densities and dimensions with a higher presence in the urban area because of irrigation use. Rural zones are located outside but within the immediate vicinity of the metropolis limits, with agricultural land and buildings scattered over wide areas.

Both metropolises are poles of industrial development, with millions of inhabitants. Their main geographic similarities and differences can be seen in Table I, and a comparison of their climate conditions is shown in Table II. They are comparable in terms of geographic location, population, and climate,

although Guadalajara has a larger population and is warmer; however, both have similar annual averages of RH and rainfall. The similarity in geography and size shared by both metropolises, and the humidity variables analyzed, allow for comparisons of their hygric behaviors (Oke et al., 2017).

Around the middle of the last century, Puebla's population began to increase rapidly, as shown in Figure 2, currently being of approximately 3.2 million inhabitants. Over the last eight decades the population growth of Guadalajara has exceeded that of Puebla (Fig. 2).

2.1 Guadalajara

The Metropolitan Zone of Guadalajara is the third most populated in Mexico, with a population of 5.3 million inhabitants and the third in relation to its concentration of industrial production, which makes it the most important industrial center in western Mexico.

Settled above the Atemajac Valley at an average elevation of 1578 masl, Guadalajara has sub-humid temperate climate conditions (López-García and Márquez-Azúa, 2018). In general, the area is predominantly flat with some undulations. La Primavera forest, located to the south-southwest, is the most important forested area within the metropolis. The Chapala lake, which is located 40 km to the south-southeast from the metropolis, is the largest in Mexico with 112 km² (Table I and Fig. 3a).

The northern and northeastern boundaries of the metropolis are the Huentitán-Oblatos canyon, where the Verde and Santiago rivers flow. The U-shaped chain of hills to the west-southwest, formed by El Cuatro (with an elevation of 282 m above the Guadalajara average of 1578 masl), Santa María de Tequepexpan (132 m) and del Tesoro (150 m), and the Venta del Astillero mountain range (its highest point at 372 m above the average level of the city) to the west, determine the behavior of local winds (Davydova-Belitskaya et al., 1999).

For the period 1996 to 2017, López-García and Márquez-Azúa (2018) found for Guadalajara that the months with fastest wind speed are March, April, and May with averages of 4.1 m s⁻¹. September, November, and December presented the lowest average speed of 2.2 m s⁻¹. According to the hourly pattern, weak gusts occur around 8:00 LT (less than

Table I. Approximate location of the studied metropolises.

Metropolis	Latitude N	Elevation (masl)	Proximity to the coast (km)	Population (millions)	Land area (km ² × 1000)	Inhabitants per km ²
Guadalajara	20.70	1578	190 of the Pacific Ocean	5.3 (IIEG, 2021)	2.6 (Gobierno del Estado de Jalisco, 2020)	2145
Puebla	19.01	2140	190 of the Gulf of Mexico	3.2 (Gobierno del Estado de Puebla, 2022)	2.4 (IMPLAN, 2021)	1431
Average	19.8	1859	190	4.3	2.5	1788

Table II. Climatological normals (1991-2019)*.

	Guadalajara	Puebla
Mean annual temperature (°C)	20.3	17.3
Annual total precipitation (mm)	940	911
Mean annual relative humidity (%)	61	58
Precipitation during May-October (%)	94	90
Coldest month (average of minimum temperature [°C])	January (6.6)	January (5.6)
Warmest month (average of maximum temperature [°C])	May (33.3)	April (27.8)

*Data source: For Guadalajara (station 14065), <https://smn.conagua.gob.mx/tools/RECURSOS/Mensuales/jal/00014065.TXT>, and for Puebla (station 21065) <https://smn.conagua.gob.mx/tools/RECURSOS/Mensuales/pue/00021065.TXT> (accessed on 2022 March 20).

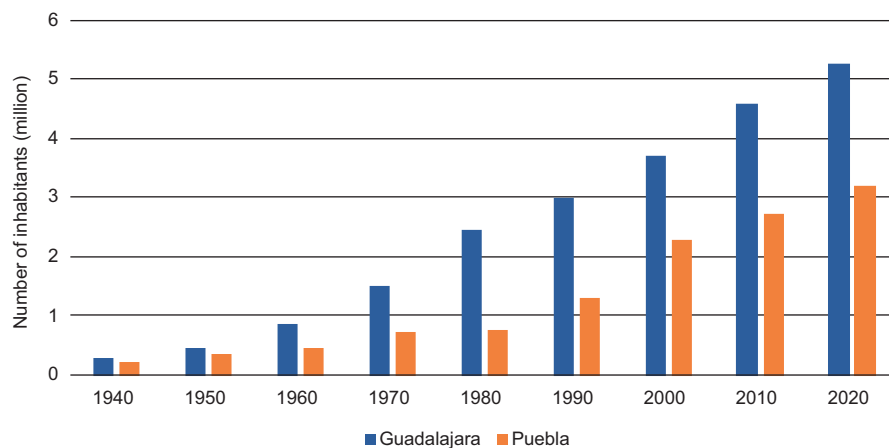


Fig. 2. Number of inhabitants of the metropolises of Guadalajara and Puebla from 1940 to 2020, according to data from the population and housing censuses carried out by IIEG (2021) and IMPLAN (2021).

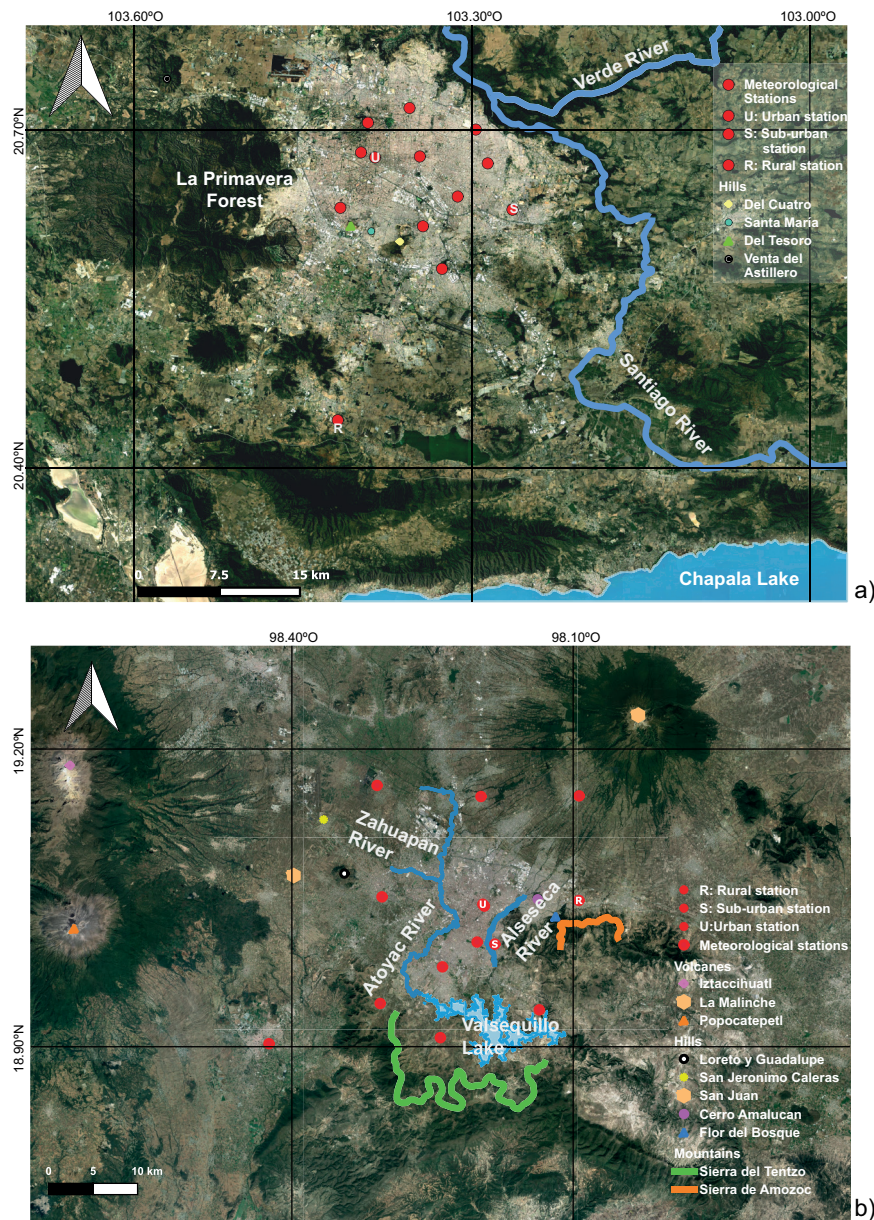


Fig. 3. Meteorological stations used to elaborate iso-hygro maps. (a) Guadalajara: IAM (urban), Loma Dorada (suburban), Tlajomulco (rural). (b) Puebla: DIAU (urban), Lomas del Mármol (suburban), Chachapa (rural).

2.0 m s^{-1}), increasing to the highest values between 18:00 and 21:00 LT (greater than 4.5 m s^{-1}). For the period 1994-1996, Davydova-Belitskaya et al. (1999) identified that west winds dominate in the dry season of the year (November-April) and east winds dominate in the rainy season, a fact that was also found by García et al. (2014) for the period 2001-2010. To provide a more detailed description of the wind

circulation in Guadalajara, 2016 was analyzed at three stations (Table III) used for this article. For winter (December, January, and February), from midnight to dawn, winds from the southeast dominated; after dawn, during the mornings, those from the east dominated; in the afternoons the dominant wind was from the west and, from nightfall to midnight, from the south. Throughout most of the spring (March,

Table III. Characteristics of the urban, suburban, and rural meteorological stations used in this work (geographical coordinates, height of sensors above street, height of roughness, land use, and waterproof surface).

	Latitude (°), longitude (°) and elevation (masl)	Height of sensors above street (m)	Height of roughness (m)	Land use	Waterproof surface (%)
Guadalajara					
IAM (urban)	20.67555 −103.38583 1583	8	0.75	Residential	80
Loma Dorada (suburban)	20.62917 −103.26389 1648	8	0.38	Residential	80
Tlajomulco (rural)	20.44222 −103.419 1566	7	0.05	Services and agricultural	10
Puebla					
DIAU (urban)	19.04365 −98.196396 2153	15	1.58	Residential	85
Lomas del Mármol (suburban)	19.00346 −98.183563 2131	8	0.24	Residential	75
San Salvador Chachapa (rural)	19.04745 −98.093872 2279	8	0.11	Agricultural and services	20

April, and May) southwesterly winds prevailed, except at night, when there were mostly westerly winds. During the six-month period from June to November the prevailing winds had an easterly component from midnight to before sunset, and from then until midnight, the wind had a westerly component.

2.2 Puebla

The economy of Puebla is based on the processing and manufacturing industries, particularly the manufacture of transportation equipment, followed by the food industry, and retail trade (42, 6, and 6% of the regional gross domestic product, respectively), concentrated in the urban and peri-urban areas, while the services sector occupies most of the city's population. The topography is flat at an average elevation of 2140 masl, with a slight slope in a northeast-south

direction of less than 3.5% (Fig. 3b). This evenness is only interrupted by low hills such as Loreto-Guadalupe, San Juan, and San Jerónimo Caleras in the northwest of the city. Important elevations also flank the city: Popocatepetl (5436 masl) and Iztaccíhuatl (5215 masl) volcanoes to the west, and La Malinche volcano (4461 masl) to the northeast, with a series of small mountain ranges (Galicia-Hernández, 2014).

The orographic conformation of the valley contributed to the formation of a hydrological system that includes a framework of groundwater flow beneath the surface slopes, which provides water for agricultural, industrial, and urban use. To the south of the urban area is the artificial lake of Valsequillo into which the Atoyac river flows, crossing the city from north to south, together with other tributary rivers such as the Alseca to the east and the San

Francisco in the central area, which is currently piped and used as drainage (INEGI, 2019).

The main sources of moisture in the area are narrow strips that follow the course of surface streams. There is also a natural protected area, Cerro de Amalucan, which is enclosed by buildings, bodies of water, cemeteries, and sports facilities, usually irrigated, especially during the dry season (see Fig. 3).

Regarding the winds in the Puebla valley, Balderas-Romero (2018) found that frequently there is calm during the night and morning until noon; between 12:00 and 18:00 LT the maximum winds are between 4 and 8 m s⁻¹. The maximum average speeds occur in April and October. The winds are characterized by symmetrical behavior: breezes from the north at night and winds from the south during daytime, with a brief period in the early evening when winds enter the valley from the east, i.e., katabatic winds (from the north) are present from 0:00 LT in winter and from 2:00 LT in spring, until 9:00 or 11:00 LT. Anabatic (south) winds start one or two hours before noon and persist all afternoon until one hour after sunset, with southerly breezes generated by the heating of the air at the bottom of the valley, contributing in the humid period to the formation of convective clouds. In the first part of the night an easterly current predominates, which is channeled towards the city through the bottleneck formed between the slopes of La Malinche and the Amozoc mountain range, and between these and the Tentzo mountain range (Fig. 3b).

3. Data and methods

The thermohygro-metric data correspond to 2016, because this year had the most complete databases from the recent decade, with Puebla having 99% and Guadalajara having 96% of useful data. In 2016, the three phases of the Southern Oscillation took place, according to the NOAA Climate Prediction Center (weak to moderate El Niño for the first four months, neutral El Niño for the next three months and weak La Niña for the last five months) (NOAA, 2022), so the results that will be described later not necessarily correspond to one of the phases. It is important to remember that the objective of the present paper is to detect urban atmospheric moisture deficits or excesses, at the limits between the canopy and the boundary layer, in comparison to the peri-urban or

rural surroundings. Therefore, the present study focuses on a local scale with the hypothesis that atmospheric phenomena on a larger scale —meso, synoptic, or global— affect the entire area comprising each metropolis in the same way.

Between the 1991-2019 climatological normals and the monthly hygric (Fig. 4) and pluvial conditions (Fig. 5) during 2016, there were no important differences in either metropolis, so the results of the 2016 analyses may be considered as typical of the respective local climates.

Figure 3a, b show the topography and the meteorological stations used to generate the iso-hygro maps, which will illustrate the present paper. Only those used for direct comparisons between different environments (urban, suburban, and rural) are listed in Table III.

The height of roughness (Z_o) shown in Table III was estimated applying the simplified method proposed by Lettau (1970), cited by Oke (1987, p. 139):

$$Z_o = 0.5 h A^*/A' \quad (1)$$

where A^* is the sum of vertical areas against the prevailing wind, obtained through 3D projection of Google Earth. Very small vegetation was not considered in this study. In the case of the trees, the area of projection of the most similar geometric body was taken (e.g., a cone projected as a triangle for a pine tree, a sphere projected as a circle for a leafy tree), but with a correction factor depending on the foliage (between 0 and 1). $A' = \pi r^2$, with $r = 500$ m, and h is the height of the canopy, which will be considered equal to that of the sensors according to Table III. Note that the values of Z_o in both metropolises are of the same magnitude, but Z_o is double for the suburban area of Guadalajara compared to the corresponding one in Puebla. In contrast, the rural area of Puebla is significantly higher than in Guadalajara.

Table IV illustrates the corresponding local climate zones according to Stewart and Oke (2012), as well as the surrounding landscapes for each meteorological station.

3.1 Instruments

In the case of Guadalajara, the urban station (Institute of Astronomy and Meteorology, IAM) corresponds to a Davis Vantage Pro 2 placed 8 m above the

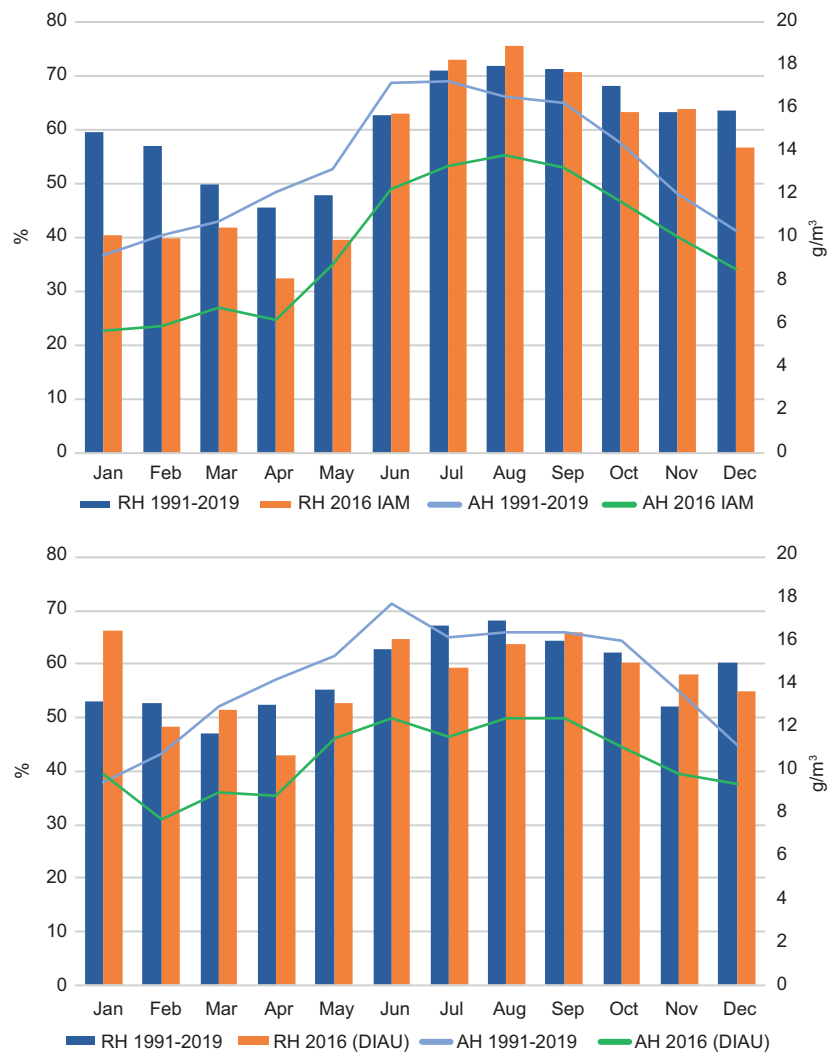


Fig. 4. Mean monthly relative humidity (RH in bars, %) for 2016 and absolute humidity (ρ_w in lines, g m^{-3}) and for the 1991-2019 normals. Upper panel: normals from station SMN 14065 vs. IAM in Guadalajara; lower panel: normals from station SMN 21065 vs. DIAU in Puebla.

ground, slightly exceeding the height of surrounding obstacles, while the suburban station (Loma Dorada) belongs to the Atmospheric Monitoring System of the Secretariat of the Environment and Territorial Development of the state of Jalisco. It measures air temperature and humidity with MetOne brand sensors at hourly frequency, and its height above street level is also 8 m, located above the rooftop of a public building without vegetation or neighboring higher buildings. The rural station (Tlajomulco) is part of the National Meteorological Service of Mexico. This station uses FTS digital sensors (model THS-2000-1)

to measure temperature and humidity, logging data every 5 min on a tower located 7 m above the ground.

The IAM station, chosen as urban station in Guadalajara, presents a high percentage of recorded data, unlike other stations near the metropolitan center. It is located at on the edge of the historic center and has experienced recent urban growth. The IAM surroundings are characterized by high economic activity; the predominant nearby constructions are buildings with two to three levels. Significant vehicular and commercial flow associated with the predominant mixed land use can be observed together with vegetation

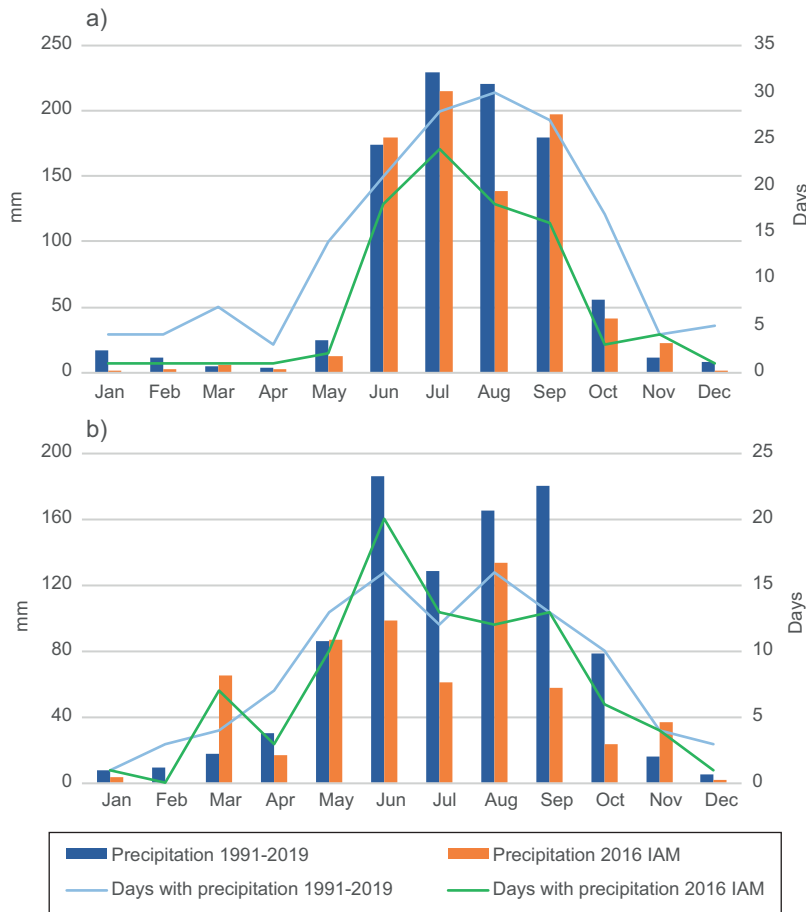


Fig. 5. Monthly precipitation for 2016 and for the 1991-2019 normals. Upper panel: normals from station SMN 14065 vs. IAM in Guadalajara; lower panel: normals from station SMN 21065 vs. DIAU in Puebla.

of tall trees of wide crowns and bushes, unlike the suburban station (Loma Dorada), as illustrated in the NDVI values in Table IV.

At the Loma Dorada station, residential land use with buildings of two to three levels and small businesses are predominant. The vegetation consists of medium-sized trees without large crowns.

Stations in Puebla differ in height among them. The DIAU station (urban) is located more than 15 m above the street level but is surrounded by higher buildings. The Lomas del Mármol station (suburban) is 6 m above the street frontage, but towards the back of the buildings, with a height of about 10 m (since it is in an area with a steep slope). The Chachapa station (rural) has an approximate height of 8 m. The three stations are Davis Vantage Pro 2 and collect data every 15 min.

The papers cited in Table SI show no uniformity with respect to the heights above the ground where the measures were taken, although most of them were located within the urban canopy. In this study, if the heights at which the measuring stations are located are compared with the respective roughness heights of their environments (see Fig. 3), it can be inferred that the urban and suburban sensors of both metropolises are at the limit between the urban canopy and the boundary layer, while the rural ones are properly at the boundary layer. Table IV shows images of a 1-km area surrounding each of the stations in Table III.

From the rural station in Guadalajara (Tlajomulco) and the three stations in Puebla, hourly averages of ambient temperature (T in $^{\circ}\text{C}$) and RH (in %) were obtained and coupled with the timetable database of the IAM and Loma Dorada stations. Figures 6, 8, 9, 11,

Table IV. Local climate zones (LCZ), texture, Normalized Difference Vegetation Index (NDVI), and vegetation profile for the three weather stations analyzed in each metropolis.

	Guadalajara			Puebla		
	Urban	Suburban	Rural	Urban	Suburban	Rural
LCZ	3 _C Compact midrise with scattered trees	6 _C Open low rise with bush/scrub	9 _F Sparsely built/ agriculture soil	2 _C Compact midrise with bush/scrub	5 _C Open midrise with bush/scrub	7 _D Lightweight with low plants
Texture						
NDVI						
Vegetation profile						

and 12 were generated using this database. For Figures 7 and 10 to 13, we derived the hourly average from the absolute humidity (ρ_w , in g m^{-3}) using the recurrence formula (Tejeda-Martínez et al., 2018):

$$\rho_w = 217 e/T_k \quad (2)$$

where e is the vapor pressure (in hPa) and T_k the temperature in absolute degrees (K), while e was obtained by clearing the definition of RH with e_s (saturation vapor pressure [in hPa] as function of temperature T [in °C]), calculated with the polynomial expression of Adem (1967), so that:

$$e = \text{RH} (6.115 + 0.42915T + 1.4206 \times 10^{-2}T^2 + 3.046 \times 10^{-4}T^3 + 3.2 \times 10^{-6}T^4) / 100 \quad (3)$$

The maps in Figure 3 were developed using the QGIS software (QGIS Development Team, 2022), geo-referencing the elements previously mentioned in the present paper. The isolines in Figures 6 and 7 were plotted using the Surfer software (Surfer, 2021), which generated a grid of 100 rows by 56 columns for Guadalajara, and a grid of 100 rows by 68 columns for Puebla. The isolines were obtained using the Radial Basis Function (RBF) interpolation method (Burrough and McDonnell, 1998), because the lines were smoother and corresponded better with different land uses, surface type, and topography of the study areas.

4. Results

The iso-hygro maps of Figure 6 indicate average excess in the urban RH of about 15 pp for Guadalajara, both

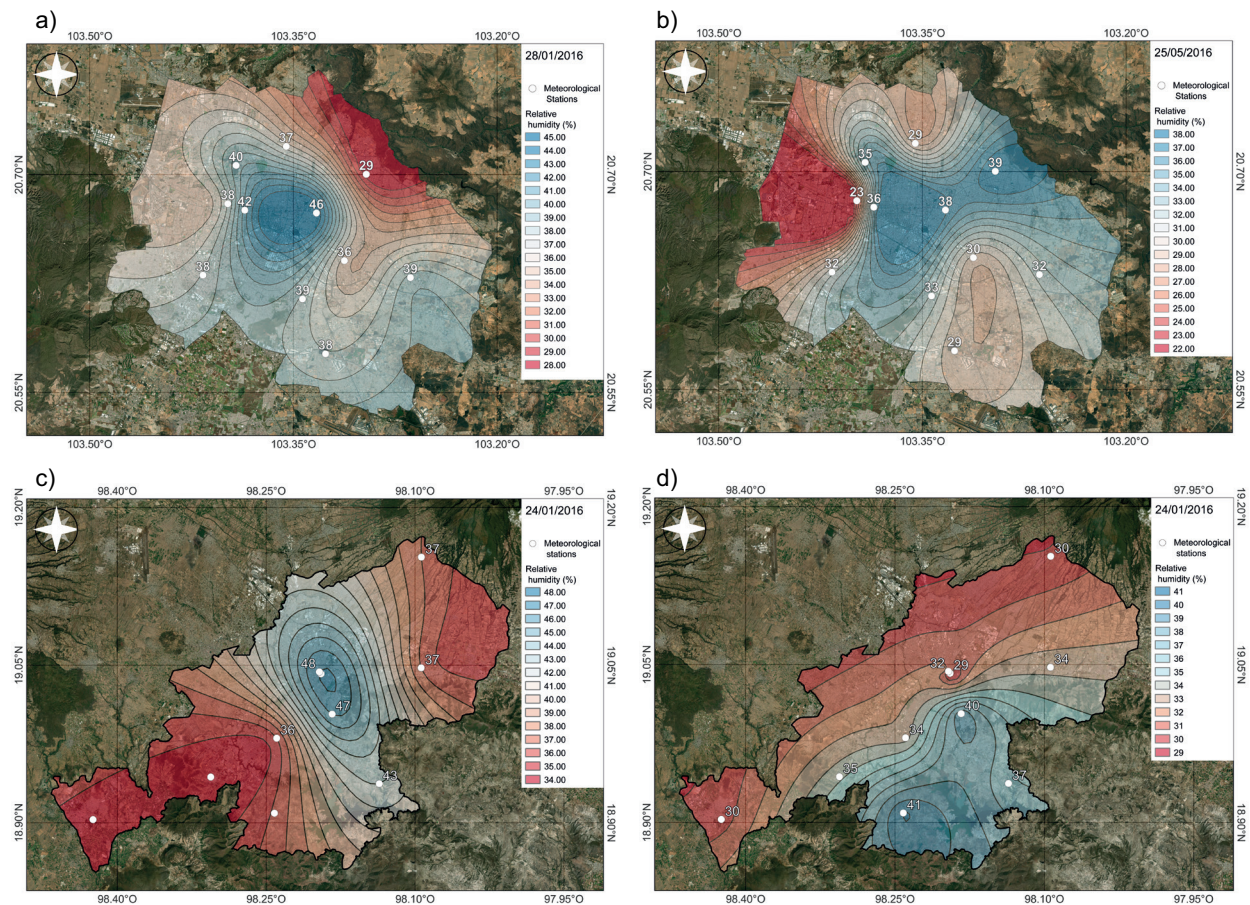


Fig. 6. Distribution of average relative humidity (%) on a cold and a warm day in 2016: (a) Guadalajara, January 28 (trough with cold front), (b) Guadalajara, May 25 (anticyclone), (c) Puebla, January 24 (high pressure associated with a cold front), (d) Puebla, May 2 (anticyclone).

for one of the coldest days and for one of the warmest in 2016. In the case of Puebla, the difference exceeds 10 pp for cold days; the influence of the urban sprawl is observed, because the highest values in the sites of higher population density are presented (Fig. 6c), while on warm days the RH is higher outside the metropolis, especially towards the sites with bodies of water (Valsequillo lake) (Fig. 6d). As it will be shown later, these average behaviors do not necessarily correspond to the hourly and daily temperature variance of these contrasts. The fact that the excess of urban RH on cold days is higher in Puebla may be because the urban canyons of the center of the metropolis are narrower than those in Guadalajara, due the irrigation of vegetation of metropolis kernel; however, it was not possible to document this with data.

Figure 7 shows the absolute humidity distribution, where an urban hygric excess from 1 to 2 g m⁻³ can be seen in both metropolises for cold days, while for warm days these differences can be up to 5 g m⁻³ and the iso-hygro maps follow the configuration of the topography. These figures show that the urban environment is, on average, more humid than its surroundings, but it must be taken into consideration that both days correspond to dry periods of the year, when irrigation is usually applied to urban gardens but not to rural surroundings.

To clarify the effects of temperature on hygric behaviors, Figure 8 shows the average hourly differences in air temperature (°C) between different environments throughout 2016. The overall urban-suburban thermal contrast in Guadalajara (Fig. 8a)

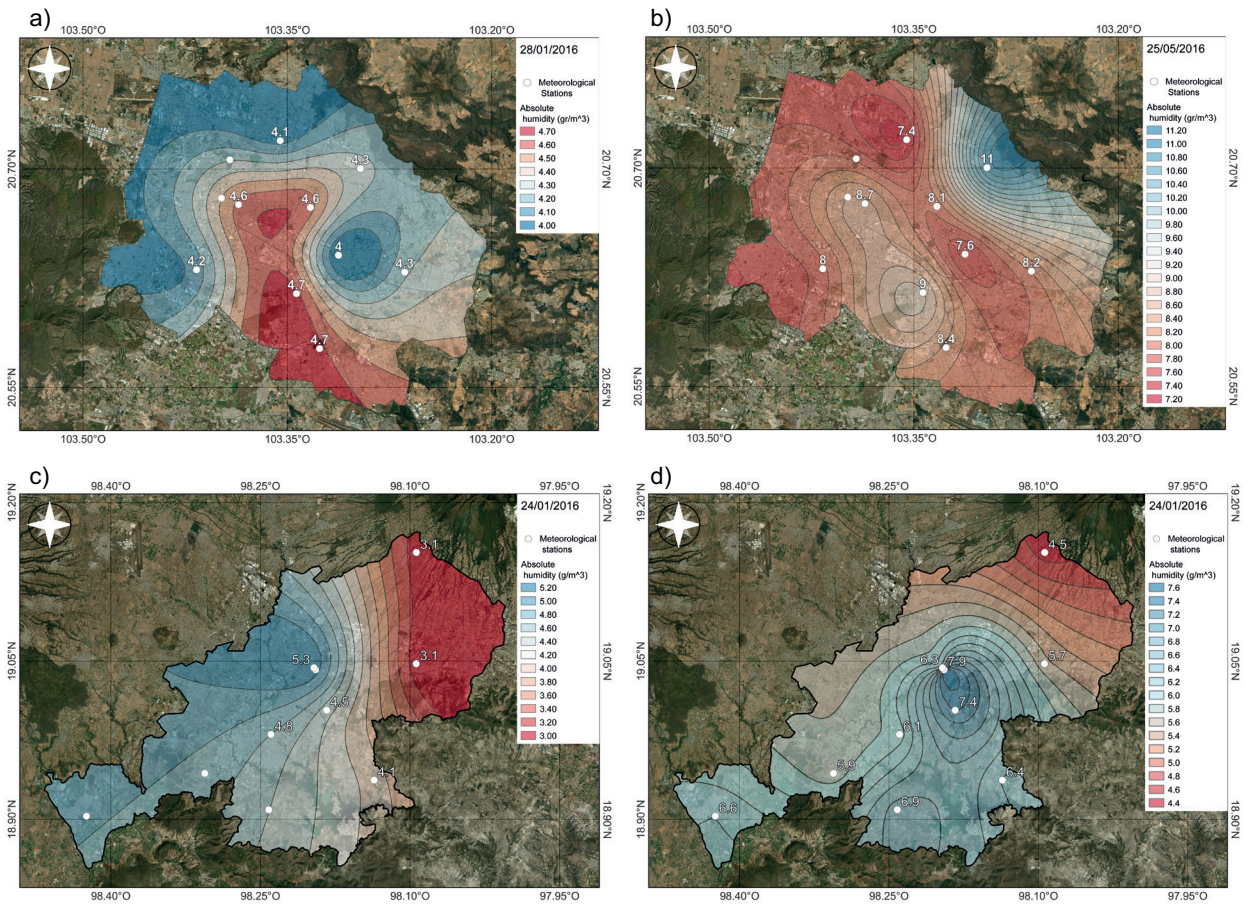


Fig. 7. Distribution of average absolute humidity (g m^{-3}) on a cold and a warm day in 2016: (a) Guadalajara, January 28, (b) Guadalajara, May 25, (c) Puebla, January 24, (d) Puebla, May 2.

is slightly positive from noon (except on some days in August, when the urban station records higher data from dawn to noon), and negative from night to noon, which is consistent with the findings of Moreyra-González et al. (2022). This is because both the IAM and Loma Dorada stations are surrounded by buildings with an average of two to three levels in height, built next to each other without spaces between them. These buildings are arranged in blocks separated by streets of varying widths, but with a greater vegetation cover in the urban station (IAM) than the suburban (Loma Dorada) as can be seen in Table IV. That is, it is possible to observe a certain similarity between the morphology and built surface density in both areas, resulting in similar thermic properties. The other three differences (Fig. 8b-d) are mostly positive during the nocturnal pe-

riods, regardless of the time year, while during daytime they are weak or even negative, with a different pattern to that observed in Figure 8a. The urban-rural contrasts are more intense (Fig. 8b, d) and with larger differences in Guadalajara (Fig 8b), where a high contrast is observed in the presence of built elements between urban and rural environments. While the urban area has a 90% waterproof environment with a densely built morphology, the rural environment shows few conglomerated buildings in isolated cores surrounded by predominantly permeable areas dedicated to agricultural use. The rural area has low density buildings with land use corresponding to municipality services or early small housing developments. In contrast, mainly in summer, the differences of positive temperatures in the urban-rural comparison in Puebla extend to several hours during the day.

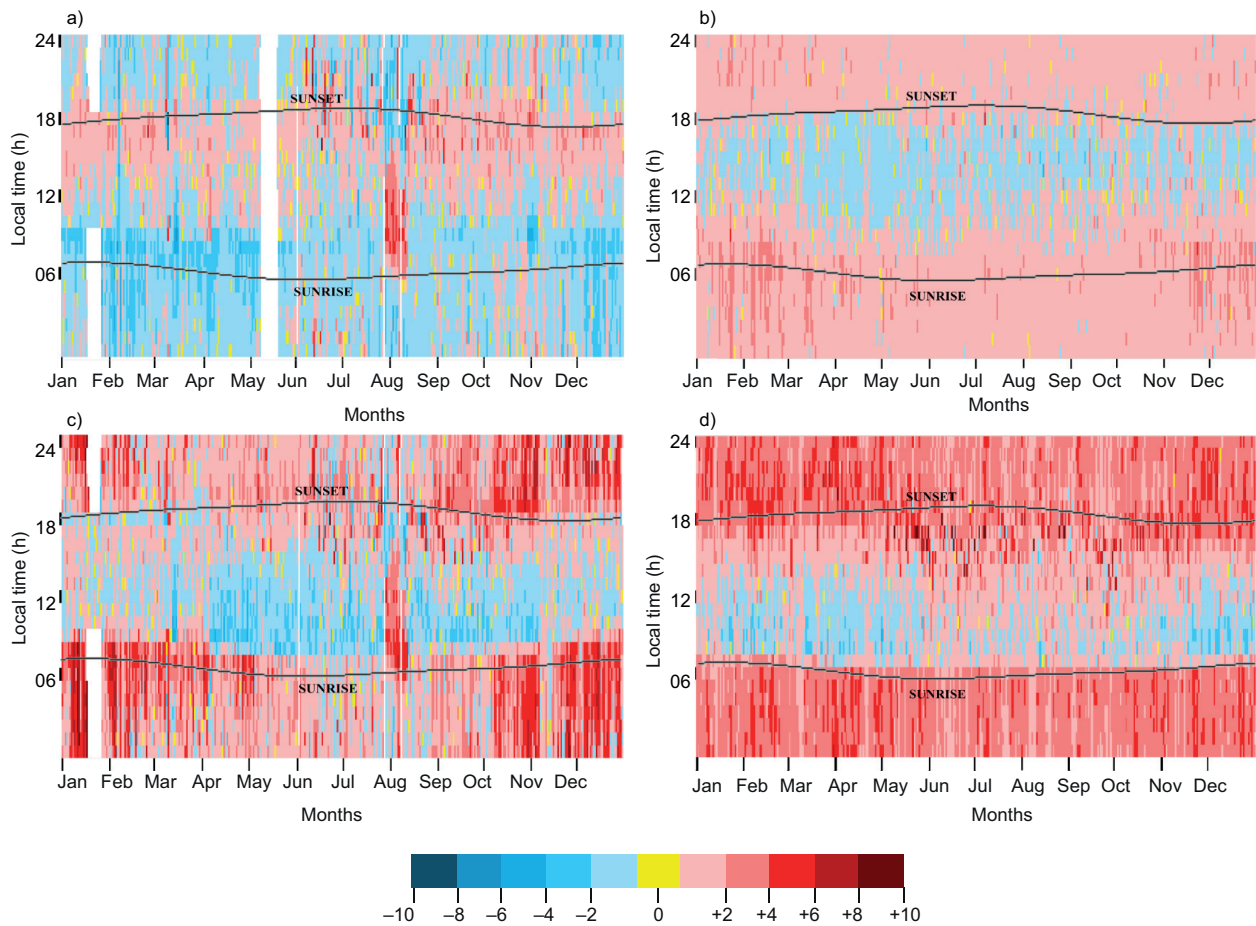


Fig. 8. Daily average differences for air temperature ($^{\circ}\text{C}$) between different environments in 2016 for: (a) urban-suburban Guadalajara, (b) urban-rural Guadalajara, (c) urban-suburban Puebla, (d) urban-rural Puebla. Months are shown on the X-axis and local time on the Y-axis.

In Figure 9, the average differences in RH (in pp) follow inverse patterns to those observed in Figure 8. i.e., there are RH deficits when urban excesses of temperature occur, as the behavior of the RH is strongly dominated by the thermal behavior, according to the Clausius-Clapeyron equation (Oke et al., 2017, chpt. 9; Tejeda-Martínez et al., 2018).

Figure 10a (urban-suburban in Guadalajara) shows how the urban excess of absolute humidity predominates from February to December. The urban-rural difference (Fig. 10b) is positive from November to June, almost regardless of the time of day. As mentioned above, artificial irrigation of vegetated areas as a source of moisture, could lead to higher evapotranspiration in urban and suburban areas than

in rural areas, where the sowing areas practically remain dry outside the rainy season. Nevertheless, it was not possible to obtain reliable information about the artificial irrigation patterns to fully confirm this. In Puebla, the urban-suburban contrasts (Fig. 10c) are all negative except in January. The urban-rural differences (Fig. 10d) are positive between 10:00 and 18:00 LT all year round, and throughout the day from January to March. With respect to magnitude, the contrast of absolute humidity between urban and rural environments is similar for both metropolises.

From figures 8 to 10 it can be estimated that about 70% of the time the urban environment is warmer (with a lower RH) than the rural one in Guadalajara, or the rural and suburban environments

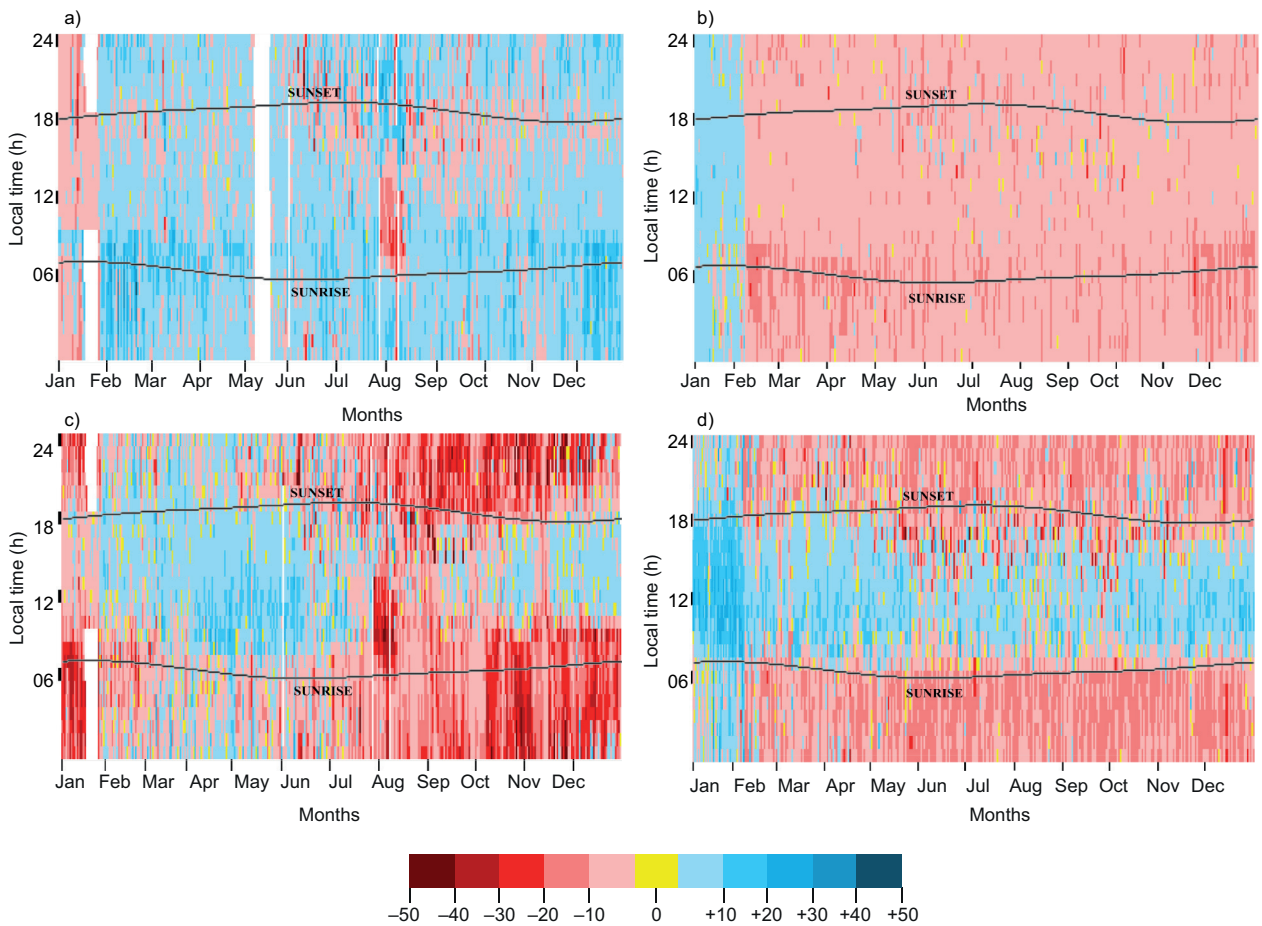


Fig. 9. Daily average differences of the relative humidity in percentage points (pp) between different environments in 2016 for both cities: (a) urban-suburban Guadalajara, (b) urban-rural Guadalajara, (c) urban-suburban Puebla, and (d) urban-rural Puebla. Months are shown on the X-axis and local time on the Y-axis.

in Puebla. In the comparison between urban and suburban environments in Guadalajara, only 34% of the time the urban is warmer and 86% of the time it has a higher RH. Most of the time, absolute humidity is higher in the urban environment, except when urban-suburban areas in Puebla are compared. On average, these differences are less than 1 gm^{-3} , which is usually within the uncertainty ranges of the measuring instruments.

Although Puebla is in the Gulf of Mexico slope, and Guadalajara is on the side of the Pacific Ocean, in both cases the anticyclonic effect from November to April is present. The rainy season usually begins in May, characterized by thunderstorms during the afternoon and early evening.

In Figures 11-13 isolines were also obtained using the RBF interpolation method. They were used to explore the role of the city in the drying of the urban atmosphere, showing four days with rain followed by four days without or scarce rain. In both locations, days after the rainy periods, the winds were weak or calm, discarding the effects of advection. Figure 11a, b shows the evolution of urban-suburban and urban-rural deficits/excesses for Guadalajara, respectively, of temperature for four days with precipitation (August 22 to 29, with 38.2 mm accumulated) followed by four days almost without precipitation (August 26 to 29, 2016 with 0.25 mm accumulated). The excess of urban temperature occurs during the evening period when comparing the urban

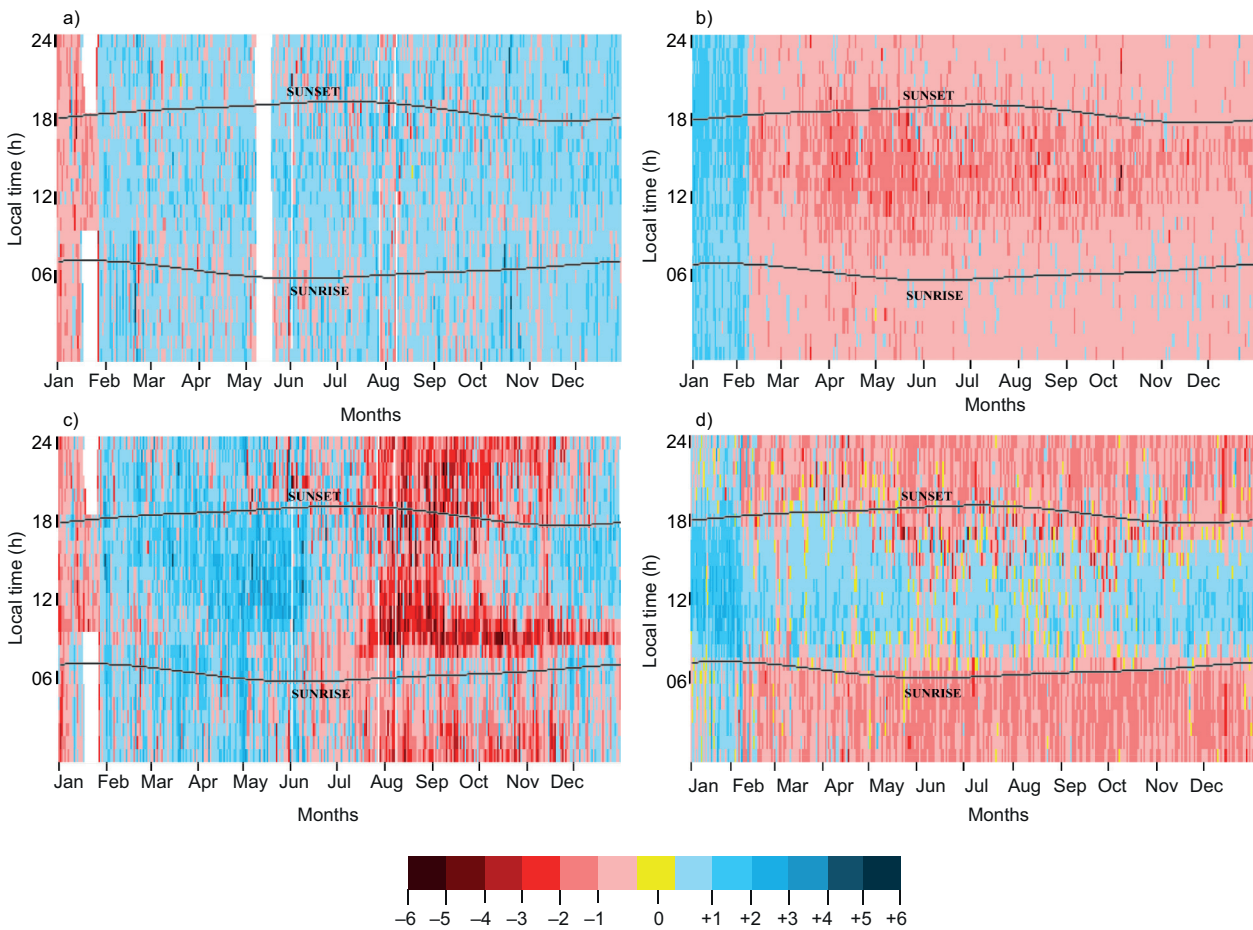


Fig. 10. Daily average differences of the absolute humidity (g m^{-3}) between different environments in 2016 for both cities: (a) urban-suburban Guadalajara, (b) urban-rural Guadalajara, (c) urban-suburban Puebla, (d) urban-rural Puebla. Months are shown on the X-axis and local time on the Y-axis.

and suburban environments (Fig. 11a), and during the evening and nocturnal periods in the urban-rural comparison (Fig. 11b). Therefore, at least in this case the rain did not have a determining effect on the urban heat island. In Puebla (Fig. 11c, d), during the four days with precipitation (August 6 to 9), 54 mm were accumulated. However, here the urban-suburban difference responds more to the daily cycle, i.e., it is negative between 12:00 and 17:00 in Figure 11c. From August 10 to 13 (2 mm accumulated) the differences intensify during the nocturnal period, especially in the urban-rural comparison (Fig. 11d), but they remain weak during the diurnal and rainy periods. This suggests that, in the case of Puebla, precipitation had an influence on the magnitude of the urban heat island, which requires further exploration in another paper.

The RH patterns shown in Figure 12 are inversely proportional to the temperature shown in Figure 11. The role of temperature over the RH is verified. On the other hand, the absolute humidity in Guadalajara (Fig. 13a) is lower at night than during day but is always positive; the urban-rural contrast (Fig. 13b) has negative values between 10:00 and 12:00 LT. In contrast, the urban-suburban differences in Puebla (Fig. 13c) are negative for the diurnal period, but positive during the urban-rural contrast for that same period throughout the year (Fig. 13d), indicating that in Puebla the suburbs could be more humid in comparison to the urban center and even more humid than the rural surroundings. However, it should be emphasized that the transition from days with precipitation to days without precipitation

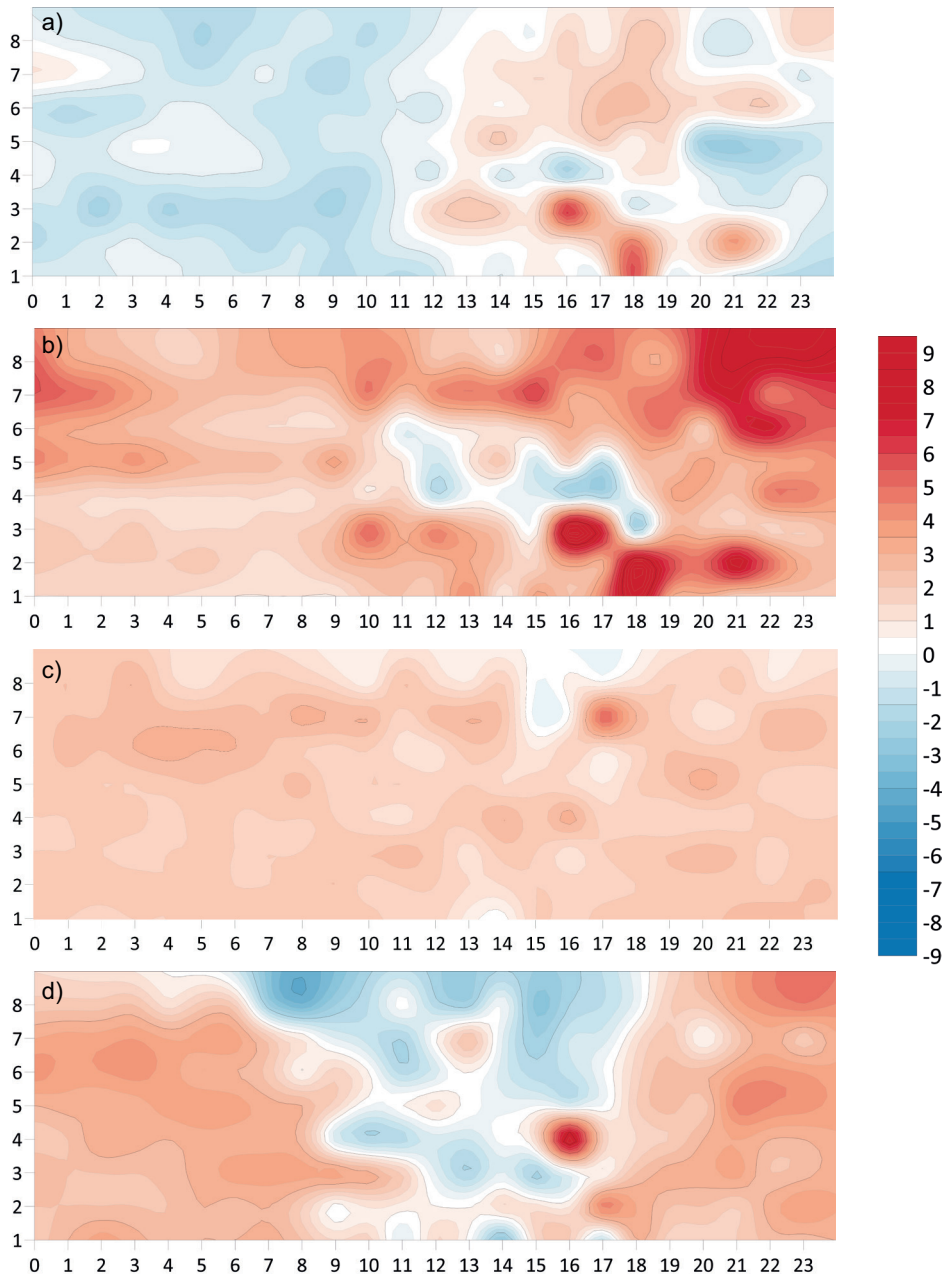


Fig. 11. Evolution of urban excesses/deficits in temperature ($^{\circ}\text{C}$) for four days with precipitation followed by four days without rain during from August 22 to 29, 2016: (a) urban-suburban Guadalajara, (b) urban-rural Guadalajara; and for August 6 to 13: (c) urban-suburban Puebla, and (d) urban-rural Puebla. Local time is shown on the X -axis and day numbers on the Y -axis.

does not show a significant impact on the contrast of absolute humidity in any of the four cases shown in Figure 13.

5. Concluding remarks

This paper describes atmospheric humidity contrasts in the limits between the urban canopy and the bound-

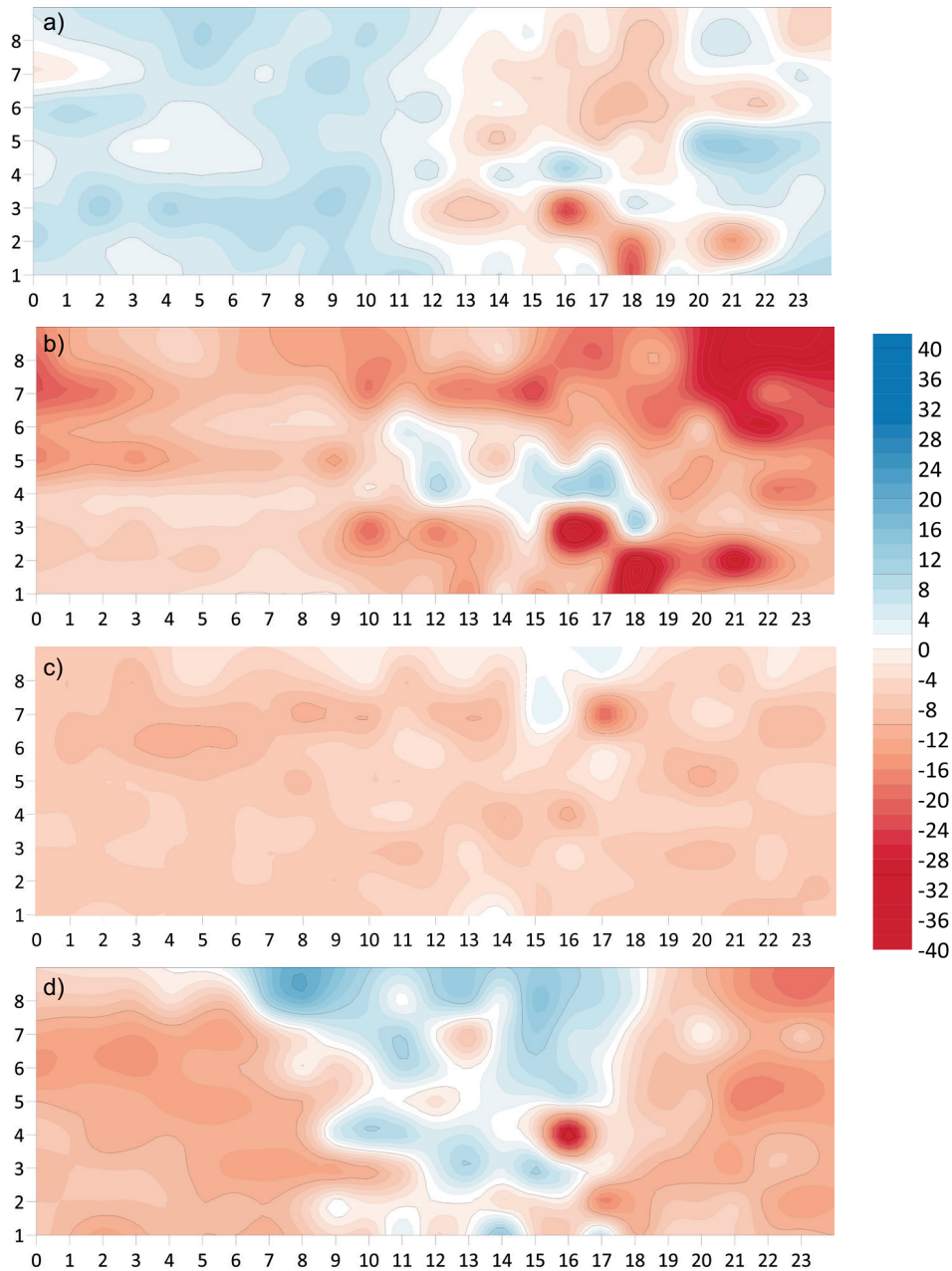


Fig. 12. Evolution of urban excesses/deficits in relative humidity (pp) for four days with precipitation followed by four days without rain during from August 22 to 29, 2016: (a) urban-suburban Guadalajara, (b) urban-rural Guadalajara; and for August 6 to 13: (c) urban-suburban Puebla, and (d) urban-rural Puebla. Local time is shown on the *X*-axis and day numbers on the *Y*-axis.

ary layer, against the corresponding ones in suburban and rural environments in two industrial high-risen Mexican metropolises with millions of inhabitants,

located in tropical latitudes. The fact that the contrasts of RH are determined by thermal differences between these environments is confirmed, which has

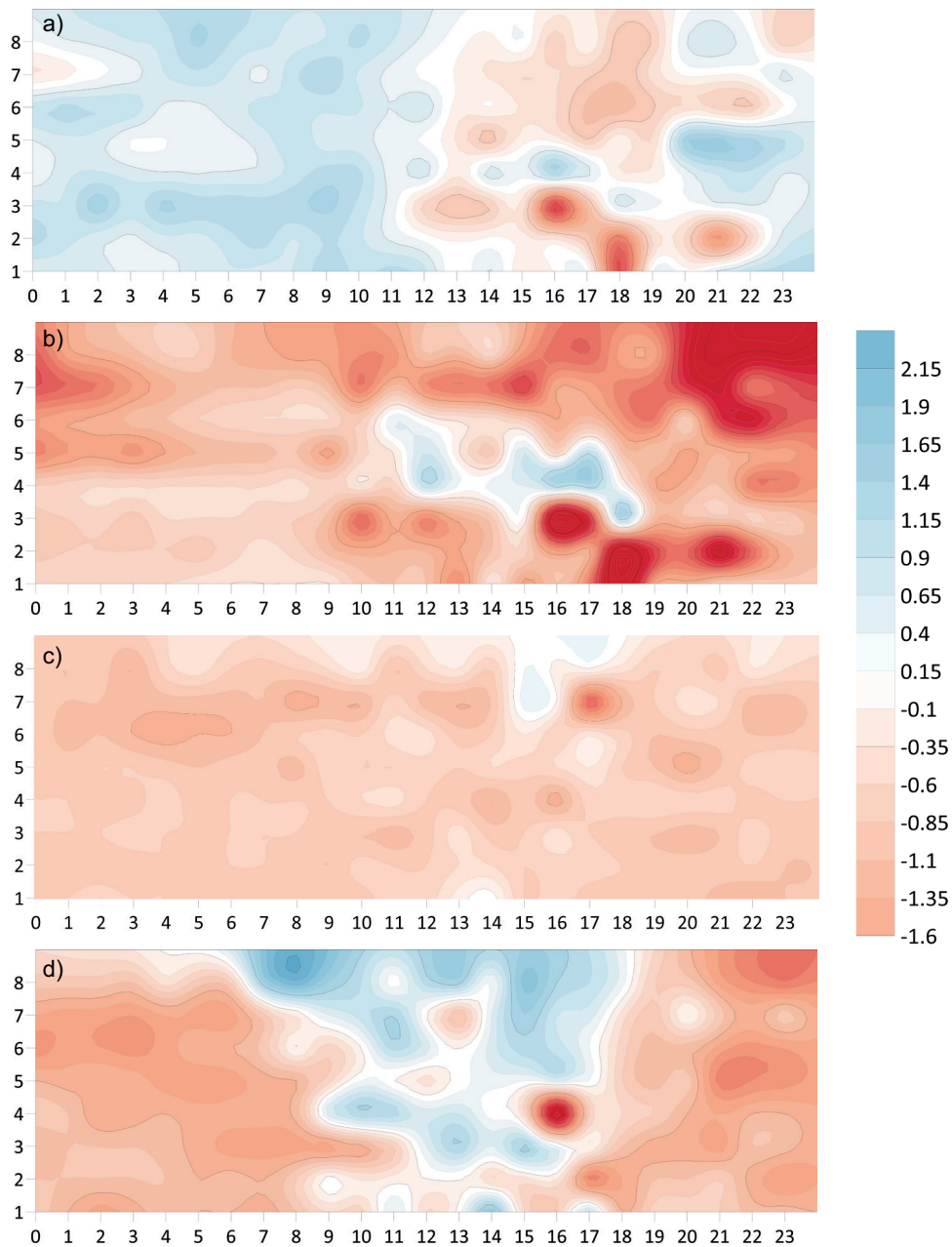


Fig. 13. Evolution of urban excesses/deficits in absolute humidity (g m^{-3}) for four days with precipitation followed by four days without rain from August 22 to 29, 2016: (a) urban-suburban Guadalajara, (b) urban-rural Guadalajara; and for August 6 to 13: (c) urban-suburban Puebla, and (d) urban-rural Puebla. Local time is shown on the X-axis and day numbers on the Y-axis.

been documented in previous works and corresponds to the inverse relation between RH and temperature according to the Clausius-Clapeyron equation.

Atmospheric humidity is important in the evaluation of human, vegetal, or animal bioclimate, so it is of interest to understand the effects of urbanization

on this climatic variable. From the present paper it can be concluded that, as urban sprawls continue to grow in Guadalajara and Puebla, urban dryness will be intensified in terms of RH, as the result of the urban heat island increment. However, for the purposes of urban planning and its relationship with bioclimate, the comparisons of absolute humidity contrasts are of major interest, since this variable measures the vapor concentration in the atmosphere. The contrasts of urban environment compared to suburban and rural areas are more intense the greater the urban sprawl. However, it is not easy to deduce a spatial or temporal pattern (annual or daily cycle) because it is a complex phenomenon (Yang et al., 2020) that comprises more factors to determine the behavior of humidity than those described in this article, not only geographic and climatic, but also the possible sources of water vapor emissions.

The results presented in this paper have uncertainties that could not be resolved because of the variability of wind direction and height differences of the sensors above ground. These uncertainties are also common in the cited articles in Table SI. One way to reduce the sources of error in the comparisons is conducting measuring campaigns at different times of the year.

As stated by Oke et al. (2017), the urban moisture deficit during the dry season, which is a result of lower vapor pressure in the city due to its impermeability, is not confirmed in any of the cities when analyzing absolute humidity. In Guadalajara, both the urban-suburban and urban-rural differences are negative during the dry months, regardless of the hour of the day, whereas in Puebla such differences are negative or weak for the diurnal period in the urban-suburban contrast and also for the nocturnal period in the urban-rural comparison, regardless of the month.

In Guadalajara, the influence of the geographical built environment is reflected in urban-rural contrasts in both temperature and absolute humidity. In the temperature contrast, the positive values at night are associated with the thermal properties of the built surfaces inside the metropolis. An absolute humidity contrast can be observed in the urban-rural environment even though the urban zone presents predominantly low NDVI values (Table IV) in comparison with the rural area. This could be due to moisture inputs from the irrigation of urban areas, which could contribute to higher water vapor content than in rural

areas (although there are no precise quantifications). A similar phenomenon was found by Unger (1999) in Szeged, Hungary.

Regarding the urban-suburban differences, the similarity in the geographical built environment characteristic of Guadalajara, does not decisively modify the contrast in temperature or in absolute humidity. This metropolis does not present high contrasts in morphology or type of surfaces due to its prevailing horizontal growth and absence of significant differences in topography. Both zones are similar with respect to land use (residential and commercial), built densities, facades of two to three levels and little garden area on the main avenues. The use of mechanical systems for climate control is not yet popular, so no anthropogenic heat contributions may have an influence in the contrasts of temperature and humidity.

Puebla's behavior is similar to that found in other cities (Oke et al., 2017), with a nocturnal heat island, lower values of RH and higher urban absolute humidity in the urban-rural comparison, but not in the urban-suburban case, where values are very close.

In both metropolises the urban-suburban comparisons are not very clear with respect to the absolute humidity behavior, due to similarities in the landscapes of both environments. According to Roth (2007), a city is more humid due to the presence of humidity sources, vegetation, or wind patterns, or less humid due to the urban heat island or local winds, so the mechanism is not yet clear.

When comparing rainy days followed by days without or almost without rain, it was not found that the patterns of the absolute humidity differences had a significant change due to the presence or absence of rain. In the case of Guadalajara, an urban absolute humidity excess in the urban-suburban comparison was observed during the eight days regardless of time, while the urban-rural difference around 10:00 LT was found to be negative and the rest of the time it was positive but low. In Puebla, negative values prevail in the urban-suburban comparison during daytime, and the opposite occurs at night for the urban-rural contrast.

Acknowledgments

To PAPIIT IN102820 and IN107123 projects of UNAM and to the following persons for their

suggestions and supporting: Pablo Elías-López, Juan Pablo Báez-Vásquez, Aranza Baruch-Vera, Jaqueline Gálvez-Vidal, René Gómez-Díaz, Adrián Álvarez-Pérez, Elisa Tejeda-Zacarías and Emmanuel Álvarez, as well as the Institute of Astronomy and Meteorology of the University of Guadalajara and the Jalisco Atmospheric Monitoring System.

References

- Ackerman B. 1987. Climatology of Chicago area urban-rural differences in humidity. *Journal of Applied Meteorology and Climatology* 26: 427-430. [https://doi.org/10.1175/1520-0450\(1987\)026%3C0427:COCAUR%3E2.0.CO;2](https://doi.org/10.1175/1520-0450(1987)026%3C0427:COCAUR%3E2.0.CO;2)
- Adebayo YR. 1987. The effect of urbanization on some characteristics of relative humidity in Ibadan. *Journal of Climatology* 7: 599-607. <https://doi.org/10.1002/joc.3370070608>
- Adebayo YR. 1991. Day-time effects of urbanization on relative humidity and vapour pressure in a tropical city. *Theoretical and Applied Climatology* 43: 17-30. <https://doi.org/10.1007/BF00865039>
- Adem J. 1967. Parameterization of atmospheric humidity using cloudiness and temperature. *Monthly Weather Review* 95: 83-88. [https://doi.org/10.1175/1520-0493\(1967\)095%3C0083:POAHUC%3E2.3.CO;2](https://doi.org/10.1175/1520-0493(1967)095%3C0083:POAHUC%3E2.3.CO;2)
- Balderas-Romero G. 2018. Flujo de aire superficial en la Zona Metropolitana Puebla-Tlaxcala. In: *Hacia una evaluación de las ciudades contemporáneas: diagnóstico y estrategias para la habitabilidad sostenible y calidad de vida* (Torres-Pérez ME, Ed.). Puebla: Red Nacional de Investigación Urbana-Mérida: Universidad Autónoma de Yucatán, 385-400. Available at: <http://urban.diau.buap.mx/publicaciones/flujo-de-aire-superficial-en-la-zona-metropolitana-puebla-tlaxcala.pdf> (accessed 2022 May 31).
- Burrough PA, McDonnell R.A. 1998. *Principles of Geographical Information Systems*. Oxford University Press, Oxford.
- Bulut Y, Toy S, Irmak MA, Yilmaz H, Yilmaz S. 2008. Urban-rural climatic differences over a 2-year period in the city of Erzurum, Turkey. *Atmósfera* 21: 121-133.
- Champollion C, Drobinski P, Haeffelin M, Bock O, Tarniewicz J, Bouin MN, Vautard R. 2009. Water vapour variability induced by urban/rural surface heterogeneities during convective conditions. *Quarterly Journal of the Royal Meteorological Society* 135: 1266-1276. <https://doi.org/10.1002/qj.446>
- Chandler TJ. 1967. Absolute and relative humidities in towns. *Bulletin of the American Meteorological Society* 48: 394-399. <https://doi.org/10.1175/1520-0477-48.6.394>
- Chow SD, Chang C. 1984. Shanghai urban influences on humidity and precipitation distribution. *GeoJournal* 8: 201-204. <https://doi.org/10.1007/BF00446468>
- Cicek İ, Türkoğlu N. 2009. The effects of urbanization on water vapour pressure in a semi-arid climate. *Theoretical and Applied Climatology* 95: 125-134. <https://doi.org/10.1007/s00704-007-0363-8>
- Cuadrat JM, Vicente-Serrano S, Saz MA. 2015. Influence of different factors on relative air humidity in Zaragoza, Spain. *Frontiers in Earth Science* 3: 10. <https://doi.org/10.3389/feart.2015.00010>
- Davydova-Belitskaya V, Skiba YN, Bulgakov SN, Martínez-Z A. 1999. Modelación matemática de los niveles de contaminación en la ciudad de Guadalajara, Jalisco, México. Parte I. Microclima y monitoreo de la contaminación. *Revista Internacional de Contaminación Ambiental* 15: 103-111.
- Demircan N, Toy S. 2019. Checking three-year differences in some climatic elements between urban and rural areas after a twelve-year period considering some effective parameters and solutions. *Fresenius Environmental Bulletin* 28: 718-725.
- Deosthali V. 2000. Impact of rapid urban growth on heat and moisture islands in Pune City, India. *Atmospheric Environment* 34: 2745-2754. [https://doi.org/10.1016/S1352-2310\(99\)00370-2](https://doi.org/10.1016/S1352-2310(99)00370-2)
- Dorighello-Tomás D. 2002. Estudio del comportamiento de la humedad relativa del aire en centros urbanos. *Boletín de la Asociación de Geógrafos Españoles* 33: 159-170.
- Dubicka M, Rosiński D, Szymanowski M. 2003. The influence of the urban environment on the air humidity in Wrocław. In: *Man and climate in the 20th century* (Pyka J, Dubicka M, Szczepankiewicz-Szmyrka A, Sobik M, Błaś M, Eds.). *Acta Universitatis Wratislaviensis* 2542, *Studia Geograficzne* 75: 504-527.
- Emmanuel R, Johansson E. 2006. Influence of urban morphology and sea breeze on hot humid microclimate: The case of Colombo, Sri Lanka. *Climate Research* 30: 189-200. <http://doi.org/10.3354/cr030189>
- Fortuniak K, Kłysik K, Wibig J. 2006. Urban-rural contrasts of meteorological parameters in Łódź. *Theoretical and Applied Climatology* 84: 91-101. <https://doi.org/10.1007/s00704-005-0147-y>

- Galicia-Hernández E. 2014. Territorio y sistema hídrico de la planicie del suroeste de Tlaxcala a través del tiempo. In: *Nativitas, Tlaxcala: la construcción en el tiempo de un territorio rural* (Salas-Quintanal H, Rivermar-Pérez ML, Eds.). UNAM, Instituto de Investigaciones Antropológicas, México, 21-36. Available at: http://www.rniu.buap.mx/edit/otros/pdf/lib_NativitasTlx_hsalas.pdf (accessed 2022 June 12).
- García M, Ulloa H, Ramírez H, Fuentes M, Arias S, Espinosa M. 2014. Comportamiento de los vientos dominantes y su influencia en la contaminación atmosférica en la zona metropolitana de Guadalajara, Jalisco, México. *Revista Iberoamericana de Ciencias* 1: 97-116.
- Giannaros TM, Melas D. (2012). Study of the urban heat island in a coastal Mediterranean City: The case study of Thessaloniki, Greece. *Atmospheric Research* 118: 103-120 <https://doi.org/10.1016/j.atmosres.2012.06.006>
- Gobierno del Estado de Jalisco. 2020. Área Metropolitana de Guadalajara. Available at: <https://www.jalisco.gob.mx/es/jalisco/guadalajara> (accessed 2022 May 21).
- Gobierno del Estado de Puebla. 2022. Sistema de Información Territorial del Estado de Puebla versión 1.0. Secretaría de Medio Ambiente, Desarrollo Sustentable y Ordenamiento Territorial, Gobierno de Puebla. Available at: <https://dduia.puebla.gob.mx/SITEP/apartados/zonaM.php> (accessed 2022 May 12).
- Hage KD 1975. Urban-rural humidity differences. *Journal of Applied Meteorology and Climatology* 14: 1277-1283. [https://doi.org/10.1175/1520-0450\(1975\)014<1277:URHD>2.0.CO;2](https://doi.org/10.1175/1520-0450(1975)014<1277:URHD>2.0.CO;2)
- Henry JA, Dicks SE, Marotz GA. 1985. Urban and rural humidity distributions: Relationships to surface materials and land use. *Journal of Climatology* 5: 53-62. <https://doi.org/10.1002/joc.3370050105>
- Holmer B, Eliasson I. 1999. Urban-rural vapour pressure differences and their role in the development of urban heat islands. *International Journal of Climatology* 19: 989-1009. [https://doi.org/10.1002/\(SICI\)1097-0088\(199907\)19:9<989::AID-JOC410>3.0.CO;2-1](https://doi.org/10.1002/(SICI)1097-0088(199907)19:9<989::AID-JOC410>3.0.CO;2-1)
- IEEG. 2021. Análisis de los principales resultados del censo 2020 de las áreas metropolitanas de Jalisco, 2010-2020. Instituto de Información Estadística y Geográfica de Jalisco. Available at: <https://ieeg.gob.mx/ns/wp-content/uploads/2021/02/AMG.pdf> (accessed 2022 May 21).
- IMPLAN. 2021. Programa Municipal de Desarrollo Urbano de Puebla, vol. III. Instituto Municipal de Planeación, Secretaría de Desarrollo Urbano y Sustentabilidad, Puebla. Available at: https://www.pueblacapital.gob.mx/images/2021/desarrollo_urbano/volumen/VOLUMEN_III_23-AGOSTO.pdf (accessed 2022 May 12).
- INEGI. 2019. Cuenca hidrológica Alto Atoyac. Humedales. Informe técnico. Instituto Nacional de Estadística y Geografía, México, 78 pp. Available at: https://www.inegi.org.mx/contenido/productos/prod_serv/contenidos/espanol/bvinegi/productos/nueva_estruc/702825189884.pdf (accessed 2022 June 23).
- Jáuregui E, Tejeda A. 1997. Urban-rural humidity contrasts in Mexico City. *International Journal of Climatology* 17: 187-196. [https://doi.org/10.1002/\(SICI\)1097-0088\(199702\)17:2<187::AID-JOC114>3.0.CO;2-P](https://doi.org/10.1002/(SICI)1097-0088(199702)17:2<187::AID-JOC114>3.0.CO;2-P)
- Kopec RJ. 1973. Daily spatial and secular variations of atmospheric humidity in a small city. *Journal of Applied Meteorology and Climatology* 12: 639-648. [https://doi.org/10.1175/1520-0450\(1973\)012<0639:D-SASVO>2.0.CO;2](https://doi.org/10.1175/1520-0450(1973)012<0639:D-SASVO>2.0.CO;2)
- Kuttler W, Weber S, Schonnefeld J, Hesselschwerdt A. 2007. Urban/rural atmospheric water vapour pressure differences and urban moisture excess in Krefeld, Germany. *International Journal of Climatology* 27: 2005-2015. <https://doi.org/10.1002/joc.1558>
- Lee DO. 1991. Urban-rural humidity differences in London. *International Journal of Climatology* 11: 577-582. <https://doi.org/10.1002/joc.3370110509>
- Langendijk GS, Rechid D, Jacob D. 2019. Urban areas and urban-rural contrasts under climate change: What does the EURO-CORDEX ensemble tell us?—Investigating near surface humidity in Berlin and its surroundings. *Atmosphere* 10: 730. <https://doi.org/10.3390/atmos10120730>
- Lettau HH. 1970. Physical and meteorological basis for mathematical models of urban diffusion processes. In: *Proceedings of Symposium on Multiple-Source Urban Diffusion Models*, US (Stern AC, Ed.). Publication No. AP-86. Air Pollution Control Office, US-EPA, Research Triangle Park, NC, 2.1-2.6.
- Li X, Fan W, Wang L, Luo M, Yao R, Wang S, Wang L. 2021. Effect of urban expansion on atmospheric humidity in Beijing-Tianjin-Hebei urban agglomeration. *Science of the Total Environment* 759: 144305. <https://doi.org/10.1016/j.scitotenv.2020.144305>
- Liu W, You H, Dou J. 2009. Urban-rural humidity and temperature differences in the Beijing area. *Theoretical*

- and Applied Climatology 96: 201-207. <https://doi.org/10.1007/s00704-008-0024-6>
- López-García AR, Márquez-Azúa B. 2018. Caracterización del régimen bioclimático humano en el Área Metropolitana de Guadalajara, México. *Revista Geográfica* 159: 29-56.
- Mayer H, Matzarakis A, Iziomon MG. 2003. Spatio-temporal variability of moisture conditions within the Urban Canopy Layer. *Theoretical and Applied Climatology* 76: 165-179. <https://doi.org/10.1007/s00704-003-0010-y>
- Moreyra-González LE, Tejeda-Martínez A, Elías-López P. 2022. Islas urbanas de calor atmosférica y superficial en Guadalajara, México. In: *Avances en el estudio de islas de calor urbano en América Latina (Lemoine-Rodríguez R, Pérez Vega Mas J-F, Eds.)*. CIGA-UNAM, Universidad de Guadalajara. In Press.
- NOAA. 2022. Cold and warm episodes by season. Historical El Niño/La Niña episodes (1950-present). NOAA-National Weather Service-Climate Prediction Center. Available at: https://origin.cpc.ncep.noaa.gov/products/analysis_monitoring/ensostuff/ONI_v5.php (accessed 2022 February 20).
- Oguntoyinbo JS. 1986. Some aspects of urban climates of tropical Africa. In: *Urban climatology and its applications with special regard to tropical areas*. Proceedings of the Technical Conference, Mexico City, 26-30 November (Oke TR, Ed.). WMO series 652. World Meteorological Organization, Geneva, 110-135.
- Oke TR. 1987. *Boundary layer climates*. 2nd ed. Routledge, London and New York, 435 pp.
- Oke TR, Mills G, Christen A, Voogt JA. 2017. *Urban climates*. Cambridge University Press, Cambridge, 509 pp. <https://doi.org/10.1017/9781139016476>
- Padmanabhamurty B. 1979. Isotherms and isohumes in Pune on clear winter nights: A mesometeorological study. *MAUSAM* 30: 134-138. <https://doi.org/10.54302/mausam.v30i1.2996>
- Padmanabhamurty B. 1986. Some aspects of the urban climates of India. In: *Urban climatology and its applications with special regard to tropical areas*. Proceedings of the Technical Conference, Mexico City, 26-30 November (Oke TR, Ed.). WMO series 652. World Meteorological Organization, Geneva, 136-165.
- QGIS Development Team. 2022. QGIS Geographic Information System (v. 3.24). Open Source Geospatial Foundation Project. Available at: <https://qgis.org> (zccessed 2022 April 10 to May 26).
- Richards K. 2005. Urban and rural dewfall, surface moisture, and associated canopy-level air temperature and humidity measurements for Vancouver, Canada. *Boundary-Layer Meteorology* 114: 143-163. <https://doi.org/10.1007/s10546-004-8947-7>
- Robaa SM. 2003. Urban-suburban/rural differences over Greater Cairo, Egypt. *Atmósfera* 16: 157-171.
- Robaa SM. 2013. Some aspects of the urban climates of Greater Cairo Region, Egypt. *International Journal of Climatology* 33: 3206-3216. <https://doi.org/10.1002/joc.3661>
- Roth M. 2007. Review of urban climate research in (sub) tropical regions. *International Journal of Climatology* 27: 1859-1873. <https://doi.org/10.1002/joc.1591>
- Saffell EM, Ellis AW. 2002. Urban-rural humidity variations in Phoenix, Arizona. *Journal of the Arizona-Nevada Academy of Science* 34: 53-62.
- SEMARNAT. 2020. Sistema Urbano Nacional. Secretaría de Medio Ambiente y Recursos Naturales, Mexico. Available at: https://apps1.semarnat.gob.mx:8443/dgeia/compendio_2020/dgeiawf.semarnat.gob.mx_8080/approot/dgeia_mce/html/RECUADROS_INT_GLOS/D1_SISTEMA_URBANO/D1_R_SIS-CDS00_01.htm (accessed 2022 July 10).
- Shun-Djen C. 1986. Some aspects of the urban climate of Shanghai. In: *Urban climatology and its applications with special regard to tropical areas*. Proceedings of the Technical Conference, Mexico City, 26-30 November (Oke TR, Ed.). WMO series 652. World Meteorological Organization, Geneva, 87-109.
- Stewart ID, Oke TR. 2012. Local climate zones for urban temperature studies. *Bulletin of the American Meteorological Society* 93: 1879-1900. <https://doi.org/10.1175/BAMS-D-11-00019.1>
- Surfer. 2021. Surfer v. 16.3.408. Windows. Golden Software. Available at: <https://www.goldensoftware.com/products/surfer> (accessed 2021 August 26).
- Tapper NJ. 1990. Urban influences on boundary layer temperature and humidity: Results from Christchurch, New Zealand. *Atmospheric Environment Part B, Urban Atmosphere* 24: 19-27. [https://doi.org/10.1016/0957-1272\(90\)90005-F](https://doi.org/10.1016/0957-1272(90)90005-F)
- Tejeda-Martínez A, Méndez-Pérez IR, Rodríguez NC, Tejeda-Zacarias E. 2018. *La humedad en la atmósfera. Bases físicas, instrumentos y aplicaciones*. Universidad de Colima, Colima, México, 263 pp. Available at: <http://ww.ucol.mx/content/publicacionesenlinea/>

- adjuntos/La-humedad-en-la-atmosfera_466.pdf (accessed 2022 June 8).
- Um HH, Ha KJ, Lee SS. 2007. Evaluation of the urban effect of long-term relative humidity and the separation of temperature and water vapor effects. *International Journal of Climatology* 27: 1531-1542. <https://doi.org/10.1002/joc.1483>
- Unger J. 1999. Urban-rural air humidity differences in Szeged, Hungary. *International Journal of Climatology* 19: 1509-1515. [https://doi.org/10.1002/\(SICI\)1097-0088\(19991115\)19:13<1509::AID-JOC453>3.0.CO;2-P](https://doi.org/10.1002/(SICI)1097-0088(19991115)19:13<1509::AID-JOC453>3.0.CO;2-P)
- Unger J, Skarbit N, Gál T. 2018a. Absolute moisture content in mid-latitude urban canopy layer, Part 1: a literature review. *Acta Climatologica* 51-52: 37-45. <https://doi.org/10.14232/acta.clim.2018.52.2>
- Unger J, Skarbit N, Gál T. 2018b. Absolute moisture content in mid-latitude urban canopy layer, part 2: results from Szeged, Hungary. *Acta Climatologica* 51-52: 47-56. <https://doi.org/10.14232/acta.clim.2018.52.3>
- Unkašević M. 1996. Analysis of atmospheric moisture in Belgrade, Yugoslavia. *Meteorologische Zeitschrift* 5: 121-124. <https://doi.org/10.1127/metz/5/1996/121>
- Unkašević M, Jovanović O, Popović T. 2001. Urban-suburban/rural vapour pressure and relative humidity differences at fixed hours over the area of Belgrade city. *Theoretical and Applied Climatology* 68: 67-73. <https://doi.org/10.1007/s007040170054>
- Wang JA, Hutyra LR, Li D, Friedl MA. 2017. Gradients of atmospheric temperature and humidity controlled by local urban land-use intensity in Boston. *Journal of Applied Meteorology and Climatology* 56: 817-831. <https://doi.org/10.1175/JAMC-D-16-0325.1>
- Yang X, Peng LLH, Chen Y, Yao L, Wang Q. 2020. Air humidity characteristics of local climate zones: A three-year observational study in Nanjing. *Building and Environment* 171, 106661. <https://doi.org/10.1016/j.buildenv.2020.106661>
- Yilmaz S, Toy S, Irmak MA, Yilmaz H. 2007. Determination of climatic differences in three different land uses in the city of Erzurum, Turkey. *Building and Environment* 42: 1604-1612. <https://doi.org/10.1016/j.buildenv.2006.01.017>

Supplementary material

Table S1. Summary of publications on urban atmospheric humidity

Urban zones	Location	Characteristics	Size	Variable	Period	Urban moisture excess	References
Leicester, UK	52° 38' N, 1° 8' W, 67 masl	English Midland City	270 000 inhabitants	e , RH	Summer 1966	+0.5 to 1 hPa (nocturnal), -10 pp nocturnal	(Chandler, 1967)
Chapel Hill, North Carolina, USA	35° 53' N, 79° 2' W, 148 masl	Humid with hot summers and freezing winters	29 000 inhabitants; 1200 km ²	e	Early fall 1971	+1 hPa (nocturnal), -1 hPa (diurnal)	(Kopeck, 1973)
Edmonton, Canada	53° 36' N, 113° 30' W, 645 masl	Dry with hot summers and freezing winters	1 159 000 inhabitants (2011); 684.37 km ²	RH , r_w	1961-1973	0 to 5 g m ⁻³ (entire year); +5 to -10 pp (summer nights)	(Hage, 1975)
Pune, India	18° 31' N, 73° 51' E, 560 masl	Tropical dry-wet (quasi-continental)	860 000 inhabitants (1971); 300 km ²	RH	Dec. 1974 and Nov. 1975	15 pp	(Padmanabhamurty, 1979)
Shanghai	31° 6' N, 121° 30' E, 4 masl	Humid subtropical	24 871 000 inhabitants (2003); 6340 km ²	e	1959	Lower in city, except nocturnal (+1 hPa)	(Chow and Chang, 1984)
Lawrence (Kansas, USA)	38° 57' N, 95° 13' W, 264 masl	Small eastern Great Plains city	48 000 inhabitants	Td	1976	On 45 dew point temperature points in summer and autumn, man-made (natural) surface materials are consistently negatively (positively) correlated with humidity	(Henry et al., 1985)
Ibadan, Nigeria	7° 24' N, 3° 53' E, 230 masl	Tropical wet-dry	2 550 000 inhabitants (2021); 3080 km ²	RH	1981	-7 pp	(Oguntoyinbo, 1986)
Delhi, India	28° 36' N, 72° 15' E, 239 masl	Subtropical-semi-arid	9 420 644 inhabitants (1991); 1483 km ²	RH	1978	+10 pp in low temperature period (February)	(Padmanabhamurty, 1986)

e : vapor pressure; q : specific humidity; Td : dew point temperature; RH : relative humidity; r_w : absolute humidity.

Table SI. Summary of publications on urban atmospheric humidity

Urban zones	Location	Characteristics	Size	Variable	Period	Urban moisture excess	References
Shanghai	31° 11' N, 121° 30' E, 11 masl	Humid subtropical	24 871 000 inhabitants (2003); 6340 km ²	e	1961-1970	+1 hPa, June and July	(Shun-Djen, 1986)
Chicago	41° 50' N, 87° 42' W, 182 masl	Dry with hot summers and freezing winters	3 million inhabitants (1980); 24 814.7 km ²	e	1963-1970	April-September: -0.08 (morning) to 0.43 hPa (afternoon)	(Ackerman, 1987)
Ibadan, Nigeria	7° 24' N, 3° 53', 230 masl	Humid tropical with wet and dry seasons	2 million, 1600 to 8000 inhabitants km ²	RH	1961-1980	-2 pp (9 am) to -10 pp (3 pm)	(Adebayo, 1987)
Christchurch, New Zealand	43° 30' S, 172° 37' E, 20 masl	Oceanic climate	390 300 inhabitants (2007); 1426 km ²	q	Winter 1978	1 g kg ⁻¹ (surface) to 0.15 at 75 m height, to 0 at 200 m	(Tapper, 1990)
London	51° 30' N, 0° 7' W, 15 masl	Oceanic climate	8 962 000 inhabitants (2019); 1572 km ²	e	1979-1988	0.2 to 1.0 hPa (nocturnal); +0.3 to -0.2 (diurnal)	(Lee, 1991)
Ibadan, Nigeria	7° 24' N, 3° 53' E, 230 masl	Humid tropical environment with two distinct, wet and dry, seasons	2 million, 1600 to 8000 inhabitants km ²	RH, e	1985-1986,	1-5 hPa (9 am) to 3-7 hPa (3 pm) diurnal	(Adebayo, 1991)
Belgrade	44° 47' N, 20° 28' E, 132 masl	Sub-continental template climate	1.2 million, 360 km ²	e, RH mean monthly	1925-1991	e invariant, and RH dropped since 1970	(Unkašević, 1996)
Mexico City	19° 30' N, 99° 5' W, 2450 masl	Wet cold	8 235 744 inhabitants (1990); 1495 km ² (2010)	q, RH	June 12 to 18, 1993	0.8 (1 am) to -0.2 (3 am, local time), g kg ⁻¹	(Jáuregui and Tejeda, 1997)
Szeged, Hungary	46° 42' N, 19° 0' E, 79 masl	Oceanic climate with cold winters, hot summers, and little rainfall	159 074 inhabitants (2010); 280.84 km ²	e	1978-1980	0.9 (January, 7 am) to 5.6 (August, 7 pm) hPa	(Unger, 1999)

e : vapor pressure; q : specific humidity; Td : dew point temperature; RH : relative humidity; r_w : absolute humidity.

Table SI. Summary of publications on urban atmospheric humidity

Urban zones	Location	Characteristics	Size	Variable	Period	Urban moisture excess	References
Göteborg, Sweden	57° 42' N, 11° 58' E, 12 masl	Oceanic climate with abundant rainfall in summer	600 473 inhabitants (2005); 203.67 km ²	e	1988-1990, 1994	1 (normal) to 7 hPa (summer nights)	(Holmer and Eliasson, 1999)
Pune City, India	30° 6' N, 31° 18' E, 560 masl	Humid and dry tropicacclimate	4 597 000 inhabitants (2005); 1109.69 km ²	e	April 1987	3 hPa (average)	(Deosthali, 2000)
Belgrade	44° 47' N, 28° 30' E, 117 masl	Continental with hot summer	1 757 000 inhabitants (2002); 359.96 km ²	e	1976-1980	+1 hPa (diurnal September-February) -1 hPa (diurnal February-September)	(Unkašević et al., 2001)
Brazil	15° 48' S, 47° 53' W, 1171 masl	Humid tropical	3 015 000 inhabitants (2016); 5802 km ²	RH	1961-1997	0 (1961) to 10 pp (1997), yearly average	(Dorighello, 2002)
Phoenix, Arizona	33° 23' N, 112° 42' W, 1086 masl	Dry with hot summers	1 446 000 inhabitants (2010); 1341.48 km ²	Td	1990s decade (14 meteorological stations)	-1 to 0 °C	(Saffell and Ellis, 2002)
Greater Cairo	18° 30' N, 73° 54' E, 23 masl	Hot desert	16 794 000 inhabitants (2013); 553 km ²	e	1995-2000	+1 hPa, average, 6 am -1 hPa, average, 2 pm	(Robaa, 2003)
Wroclaw, Poland	51° 6' N, 17° 1' E, 11 masl	Humid continental climate	600 000 (200); 290 km ²	e	2001	-1.9 hPa (summer) to -0.5 hPa (winter)	(Dubicka et al., 2003)
Munich, Germany	48° 6' N, 11° 35' E, 519 masl	Subpolar oceanic climate	1 562 000 inhabitants (2019); 310.74 km ²	e	August 1981, January 1982	+1 hPa (August), +0.1 hPa (January)	(Mayer et al. 2003)
Vancouver, Canada	49° 12' N, 123° 5' W, 152 masl	Oceanic climate	2 208 300 inhabitants (2011); 310.74 km ²	q	Summer 1996	Mean 0.5 gm ⁻³	(Richards, 2005)

e : vapor pressure; q : specific humidity; Td : dew point temperature; RH : relative humidity; r_w : absolute humidity.

Table SI. Summary of publications on urban atmospheric humidity

Urban zones	Location	Characteristics	Size	Variable	Period	Urban moisture excess	References
Lodz, Poland	51° 42' N, 19° 23' E, 278 masl	Humid continental climate	1 100 000 inhabitants (2018); 293.25 km ²	e , RH	1997-2002	-40 pp approx.; -4 hPa to 5 hPa	(Fortuniak et al., 2006)
Colombo, Sri Lanka	6° 54' N, 79° 52' E, 1 masl	High building density with high green cover and many low-rise buildings.	0.65 million inhabitants	e , RH , r_w	April 30 to May 16, 2003	-5 pp to +15 pp (clear days); -3 hPa (mid-day) 1 hPa (6 am)	(Emmanuel and Johansson, 2006)
Krefeld, Germany	51° 19' N, 6° 30' E, 39 masl	Continental	237 984 inhabitants (2007); 137.77 km ²	e	Nov. 2001 to Oct. 2002	0 (winter nights) to -0.5 hPa (diurnal summer)	(Kuttler et al., 2007)
Busan, Korea	35° 6' N, 129° 1' E	Coast temperate climate, fringe of Southeastern of the peninsula/	3 367 334 inhabitants (2019); 769.83 km ²	RH	1905-2003	-5 pp/100 years	(Um et al., 2007)
Seoul, Korea	37° 34' N, 126° 58' E	Inland basin: continental climate, lower temperatures compared to similar latitudes	25 620 000 inhabitants (2019); 605.25 km ²	RH	1905-2003	-8 pp/100 years	(Um et al., 2007)
Erzurum, Turkey	39° 53' N, 41° 17' E, 1850 masl	The city is far from the marine effect and has continental climate.	367 000 inhabitants	RH	1998-2003	-3.4 pp annual average	(Yilmaz et al., 2007)
Erzurum, Turkey	39° 53' N, 41° 17' E, 1850 masl	Continental climate.	367 000 inhabitants	RH	2003-2004	-2.5 pp annual average	(Bulut et al., 2008)
Beijing	39° 53' N, 116° 24' E, 43 masl	Humid continental climate with hot summers	21 710 000 inhabitants (2013); 16801 km ²	e , RH	1981-1997	+1.5 hPa, -6.3 pp	(Liu et al., 2009)

e : vapor pressure; q : specific humidity; Td : dew point temperature; RH : relative humidity; r_w : absolute humidity.

Table SI. Summary of publications on urban atmospheric humidity

Urban zones	Location	Characteristics	Size	Variable	Period	Urban moisture excess	References
Paris	48° 47' N, 2° 17' E, 33 masl	Oceanic climate with abundant rainfall	12 292 000 inhabitants (2015); 105.4 km ²	q and precipitable water	May and June 2004	-0.18 to +0.83 g/ kg; + 1.5 kg m ⁻²	(Champollion et al., 2009)
Aksaray, Turkey	38° 23' N, 34° 03' E, 960 masl	Oceanic climate	140 000 inhabitants	e , RH , r_w	1966-2006	0 (winter) to 1.5 hPa (summer)	(Cicek and Türkoglu, 2009)
Thessaloniki, Greece	22° 57' N, 40° 38' E, 50 masl	Mediterranean with hot and dry summers, mild and wet winters	800 000 inhabitants	e	2008-2009	0 to 1.3 hPa	(Giannaros and Melas, 2012)
Greater Cairo Region	18° 30' N, 73° 54' E, 23 masl	Subtropical climatic conditions. inhabitants in the period	12 to 19 million inhabitants in the period	RH	1990-2010	-13.9 pp	(Robaa, 2013)
Zaragoza, Spain	41° 38' N, 0° 52' W, 280 masl	Mediterranean climate, with a strong continental influence.	670 000 inhabitants	RH	2011-2012	-5 pp average	(Cuadrat et al., 2015)
Boston	42° 17' N, 71° 5' W, 146 masl	Humid subtropical climates	4 522 858 inhabitants (2008); 232,14 km ²	.	2011	0 to -7 hPa	(Wang et al., 2017)
Szeged, Hungary	46° 42' N, 19° 0' E, 79 masl	Oceanic climate with cold winters, hot summers, and little rainfall	159 074 inhabitants (2010); 280.84 km ²	e , r_w	2014-2019	0.9 to at 7 hPa	(Unger et al., 2018b)
Erzurum, Turkey	39° 53' N, 41° 17' E, 1850 masl	Continental climate.	367 000 inhabitants	RH	2002-204, 2014- 2016	-2.5 pp, -5 pp	(Demircan and Toy, 2019)
Berlin	52° 30' N, 13° 18' E, 34 masl	Oceanic climate	3 769 00 inhabitants (2019); 891.69 km ²	q , RH	2070-2099 vs 1971-2000	0.50 to 0.75 g kg ⁻¹ ; + 5 pp	(Langendijk et al., 2019)

e : vapor pressure; q : specific humidity; Td : dew point temperature; RH : relative humidity; r_w : absolute humidity.

Table S1. Summary of publications on urban atmospheric humidity

Urban zones	Location	Characteristics	Size	Variable	Period	Urban moisture excess	References
Nanjing, China	32° N, 118° E, 20 masl	Built-up areas and surrounding farmlands lie in the plains, with elevations ranging from 7 m to 30 m.	6.96 million inhabitants	RH	2016	0 to -15 pp	(Yang et al., 2020)
Beijing-Tianjin-Hebei urban agglomeration	39° 6' N, 117° 12' E, 320 masl	Humid continental climate with hot summers	106 910 000 inhabitants (2013); 216 501 km ²	e , q , RH	1961-2014 (133 meteorological stations)	Maximum decadal trends (spring) of -0.237 hPa, -0.151 g kg ⁻¹ , -1.159 pp (winter)	(Li et al., 2021)

e : vapor pressure; q : specific humidity; Td : dew point temperature; RH : relative humidity; r_w : absolute humidity.